AN ABSTRACT OF THE THESIS OF

Garold E. Radke for the degree of Master of Science in Chemistry presented on December 15, 1983

Title: Integration Methods for Enzymatic Analysis Response Curves Which Show Maxima, Minima, or Inflections

Redacted for Privacy

Abstract approved: Lawrence C. Thomas

Integration methods for enzymatic reactions were applied to transducer response vs. time curves which exhibit maxima, minima or inflections. The difference between the integral of the time dependent response and the initial response, often zero, is related to the initial enzyme activity or substrate concentration. Fluorescence response curves which exhibit a maximum due to pre- and post-filter effects at elevated concentrations of a time dependent fluorescence indicator species result in integrals which may not be unique to one analyte concentration. It was found that augmenting the integral data with the time of the maximum permitted correlation of each integral with a unique analyte concentration or enzyme activity. Integrals of response curves which exhibit minima also correlate with unique analyte concentrations. At increased concentration of analyte, however, the minimum may broaden into a minimum plateau and the time of the minimum may supplement the integral data

as a more sensitive measure of analyte concentration. Integrals of enzymatic response curves with inflection points correlate with unique analyte concentrations.

Integration methods were applied to both real and ideal systems. Theoretical rate equations were used to generate families of idealized response curves exhibiting maxima, minima and inflections. Curves were generated at either fixed initial substrate concentration with variable enzyme activity or at fixed initial enzyme activity with variable substrate concentration. Difference integrals were calculated and plotted as a function of initial substrate concentration or initial enzyme activity.

Enzymatic analyses were also performed using systems which produce families of response curves exhibiting maxima, minima and inflections. Difference integrals were calculated for these curves and related to initial enzyme activity or substrate concentration.

Integration Methods for Enzymatic Analysis Response Curves Which Show Maxima, Minima or Inflections

by

Garold E. Radke

A THESIS

submitted to

Oregon State University

in partial fulfillment of
the requirements for the
degree of

Master of Science

Completed December 15, 1983

Commencement June, 1984

APPROVED:

Redacted for Privacy

Professor of Chemistry in charge of major

Redacted for Privacy

Head of department of Chemistry

Redacted for Privacy

Dean of Graduate School

Date thesis is presented: December 15, 1983

Typed by WORD PROCESSING SPECIALISTS for Garold E. Radke

ACKNOWLEDGEMENTS

I wish to express my gratitude to my wife, Nancy for her support and patience during the course of this research. I also wish to acknowledge my brother, Bruce, and Tektronix for making available the computer used in this research. Bruce was also invaluable as a source of technical information relating to the operations and repair of the computer and associated hardware. His patience while answering innumerable questions is sincerely appreciated. I also wish to thank Larry Thomas for his optimistic support of this work.

TABLE OF CONTENTS

TABLE OF CONTENTS
(Continued)

LIST OF FIGURES

LIST OF FIGURES

LIST OF TABLES

INTEGRATION METHODS FOR ENZYMATIC ANALYSIS RESPONSE CURVES WHICH SHOW MAXIMA, MINIMA, OR INFLECTIONS

I. INTRODUCTION

Assays for enzyme activity and determinations of substrate concentrations have become increasingly popular. Implementation of computer-assisted data acquisition for rapidly changing enzymatic signal responses and the use of enzymes for diagnoses of illnesses have contributed to the popularity and to the number of enzymes and substrates currently being determined.

A common use of enzymatic analyses has been as a diagnostic tool in clinical chemistry with an estimated 25% of the clinical chemistry laboratory workload devoted to enzymatic analyses (1). Frequently, changes in the concentrations of specific enzymes in plasma or body tissues are indicative of disease or tissue damage (2). For example, enzymatic assays have been developed which assist in the diagnosis of myocardial infarction (1), several liver diseases (3,4), muscular dystropy (4), several carcinoma types (1), and pernicious anemia (5). Similarly, the concentration of DNA adducts, carcinogen metabolites bound to DNA which can be related to the tumor response, are frequently found to form according to kinetics which are more complicated than first order (6) and may be determined by enzymatic methods.

The use of enzymatic analyses in food processing is also important and includes glutamate-oxaloacetate transaminase (GOT) assays in meats to differentiate fresh meat from thawed frozen meat (4). In addition, the beverage industry uses enzymatic analyses to test for ethanol, CO_2, malic acid, lactate, glycerol and carbohydrates (7) and dairy industries check the effectiveness of pasteurization by assaying alkaline phophatase (8,9).

Historically, assays for substrate concentration were performed by equilibrium methods (10). These methods require an enzyme catalyzed reaction to attain equilibrium before monitoring the substrate related signal response. However, the need to determine enzyme activities led to development of kinetic or rate methods. Kinetic methods of analysis have been reviewed (11-13) and include those methods which monitor the transducer response signal or changes in the signal prior to the reaction achieving equilibrium.

Many kinetic methods monitor only the linear portion of the transducer response vs. time curve, usually during the first moments of the reaction while the kinetics are zero order or psuedo first order. Enzyme catalyzed reactions, however, frequently show higher order kinetics and a concomitant nonlinear response curve. In addition, response curves may also exhibit maxima, minima or inflection points at increased concentration of indicator species or as a result of coupled reactions. Currently there are at least two kinetic methods which may be used for assays involving nonlinear

response curves. These include regression and integration methods and will be discussed later. Attempts to utilize kinetic data from curves having maxima, minima or inflections, however, have not been reported.

This research applies an integration method to complicated response curves, i.e., curves which exhibit maxima, minima and inflections. Response curves are integrated over a fixed time interval which includes the maxima, minima or inflections and the difference integral is related to enzyme activity or substrate concentration. Difference integrals are calculated from the difference between the integrals of the initial response and the time dependent response.

Enzymatic systems and analytical instruments were selected based upon the shape of the resulting response curve. Reactions which employ dehydrogenase enzymes and produce reduced nicontinamide-adenine dinucleotide (NADH) as an indicator species were monitored with fluorescence techniques and resulted in a maximum in the signal response at elevated concentrations of the time dependent indicator species. Similarly, the time dependent concentration of O_2 in solution was monitored by an amperometric O_2 sensor during a reaction in which glucose is oxidized in the presence of glucose oxidase. A minimum occurs when glucose is nearly depleted and the rate of diffusion of O_2 into the solution from the surrounding environment exceeds the rate of enzymatic depletion of glucose. In a

third system, enzymatically catalyzed consecutive reactions were coupled and the absorbance of the indicator species, reduced nicotinamide-adenine dinucleotide phosphate (NADPH) was monitored. The induction period during the first few moments of the reaction is followed by a rapid increase and subsequent leveling off of NADPH concentrations resulting in response curves having inflection points.

Response curves were generated from theoretical rate equations to demonstrate the application of this method to curves not affected by significant amounts of noise and instrumental error. Assays of real systems were also performed.

Overview of Kinetic Methods

Kinetic methods of analysis relate a rate dependent measurement to the concentration of substrate species or activity of an enzyme. This differs from equilibrium methods (14) which measure a response signal after the reaction has come to equilibrium. Since enzymes affect the kinetics but not the thermodynamics of a reaction, enzyme activities can only be assayed by kinetic methods whereas substrates may be determined by either method (11).

Instrumentation technology prior to the 1960's made equilibrium methods a favorable choice over kinetic methods (11). However, with the advent of inexpensive computers, more efficient temperature

control and increasing use of enzymes in the diagnosis of illnesses, kinetic methods improved in reproducibility and gained popularity.

Kinetic methods offer several advantages over equilibrium methods (15,16). The requirement for equilibrium often results in lengthy analysis times and excesses of costly enzymes to speed the reactions to equilibrium. In addition, severe inhibition by products may slow the reaction to a stop, making pretense to equilibrium. Kinetic methods, on the other hand, are rapid since they monitor the signal prior to the reaction reaching equilibrium.

Many kinetic methods calculate the difference between rate measurements, thus cancelling the effect of blank and background signal. In addition, kinetic methods are the only way to determine enzyme activity and the effect of inhibitors and activators. Strict control of experimental conditions such as pH, ionic strength and temperature are required, however, since these conditions affect the reaction rate.

Kinetic methods are often classified according to the signal monitoring technique used (11,15). These methods include fixed-time (17-22) variable-time (18,20,22-24), one-point (25), two-point (17), continuous derivative (26-33), signal stat (34-37), integration (38), integration for signal averaging (16,19-21,39,40), regression (41-46), and differential (47-49) methods.

Several kinetic methods use fixed-time (17-22) or variable-time (18,20,22-24) procedures. With fixed-time measurements, transducer

signals are monitored during the same predesignated time interval and the change in response is related to catalytic activity or substrate concentration. Variable-time measurements measure the time required for transducer responses to attain a predetermined change in value. The elapsed time is related to catalytic activity or substrate concentration.

The simplest kinetic method in terms of measurements is the one-point method (25). With this method transducer signals are sampled at the same time during each of a series of runs and the magnitude of the signal is related to enzyme activity or substrate concentration. Modern instrumentation has nearly rendered this technique obsolete (15). With two-point methods (17) the difference between responses measured at two different times of each run is related to catalytic ability or substrate concentration.

Continuous derivative methods (26-33) calculate the initial reaction rate from an estimate of the first derivative over a portion of the response vs. time curve. The reaction rate is then related to catalytic ability or substrate concentration with a calibration plot. Techniques for approximating derivatives include use of analog circuitry (30,37), digital methods, and a graphical method of tangents (33,33). Frequently a second derivative is approximated to determine the linear portion of the response curve (11).

With signal-stat or fixed sensor methods (34-37) experimental conditions are altered to make the response signal constant. For example, in an assay for catalase (35), a H_2O_2 substrate is added to a catalase solution at an electronically controlled rate to maintain a constant substrate concentration. The constant concentration of substrate helps assure initial rate conditions throughout the assay and the total amount of substrate added over a fixed time period is directly proportional to the enzyme activity (35). Similar analyses may be performed for continuous flow analyses by varying the flow rate of a reagent stream (34,36). Since many enzyme catalyzed reactions consume or produce H^+, pH-stats are particularly amenable to these analyses. With this method the pH is maintained at a constant value by the addition of H^+ or OH^- and the rate at which the titrant is added is related to the reaction rate (36,37).

Integration methods for signal averaging (16,19-21,39,40) were developed to reduce the effects of noise by averaging noise over the integration period (40). In the fixed-time mode the linear portion of the response curve is integrated over two equal time intervals; the intervals may be consecutive or separated in time. The difference between the two integrals is then related to the reaction rate.

An integration method for more general application, including nonlinear response curves, has been introduced by Thomas (38). With this method the difference between the integral of the initial

response and the time dependent response is related to catalytic activity or substrate concentration.

With regression methods (41-46) a collection of data points are fit to a predetermined mathematical function of response vs. time. The function is usually derived from a Michaelis-Menten rate equation and may describe other than linear first order processes (42-44). Initial and equilibrium signal response and rate constants may be calculated using the "best fit" of the measured time dependent signal response and rate data (45,46). Advantages reported for this method include reduced sensitivity to variations in temperature and enzyme activity (46) and an increased dynamic range over concentrations greater than the Michaelis-Menten constant (41). For the method to be accurate, however, the reaction kinetics must satisfy the kinetic model chosen.

Differential reaction rate methods (47-49) exploit a difference in reaction rate of several species in order to simultaneously determine the concentration of two or more species. With one technique (47) several reactants produce a common product and the change in signal response due to the time dependent concentration of product over a steadily increasing time intervals is plotted as a function of the time interval. The initial concentrations of the reactants are determined by solving simultaneous equations of product response. Other methods measure the time resolved signal response

(48) or the change in response (49) due to products arising from different kinetics and therefore at different times.

Historical Development of Integration Methods

There currently exist two categories of integration methods between which a distinction is not clearly present in the literature (11,15). With one method (16,19-21,39,40) the effect of noise is reduced by averaging the signal over two intervals of the linear response curve. This is an extension of two point methods and uses integration to enhance precision of the rate data via averaging (40).

The signal averaging integration methods for enzymatic analyses were developed first in 1968 (40). Analog instruments were constructed which used operational amplifiers to integrate an input signal over two fixed time intervals and the difference between the integrals was related to the reaction rate. Ingle and Crouch introduced a fixed-time digital integration procedure in 1970 (19). A voltage to frequency converter was connected to an up-down counter and the difference in the number of counts accumulated over two identical time intervals was related to the reaction rate. Instrumental improvements for integration methods included automated mixing and sampling (16) and interfacing a microcomputer to a ratemeter (39) to control the timing of the ratemeter. Application

of signal averaging integration methods is restricted to reactions having elementary kinetics or to initial rate measurements.

In 1975 Thomas (38) described an integration method which permitted integration of nonlinear response curves arising from second order and higher kinetics. With this method a signal is integrated over a fixed time interval and a difference integral is calculated by subtracting the initial response integral, often zero, from the integral of the time dependent response. The difference integral was shown to be related to the initial enzyme or substrate concentration. A theoretical presentation of this method (38) demonstrated its applicability to enzyme systems producing nonlinear response curves.

Enzymes

International Activity Units

For theoretical rate equations molar concentrations or total moles of enzyme are often used since the enzyme is assumed to be totally pure and ideal. However, the catalytic ability of an enzyme may change with time and often is not related in a predictable fashion to the total mass of protein. Activity units, therefore, are used to quantify viable enzymes. An activity unit is an experimentally determined value. One unit is defined as the quantity of

enzyme required to catalyze one micromole of substrate per minute under specified conditions (usually optimal and 25°C).

Enzyme Kinetics

Many of the response curves studied in this research were generated from theoretically derived rate equations. The derivation of these rate equations and evaluation of constants was accomplished by others (50-53) using kinetic models for enzyme systems. These models originate from attempts to understand the mechanisms of enzyme reactions.

A nascent mechanistic understanding at the turn of the century was fathered by Brown (54,55) and Henri (56) who first suggested the formation of an enzyme-substrate complex as an intermediate step in an enzyme catalyzed reaction. The development of subsequent knowledge of enzyme kinetics centers around this pertinent assumption. Henri (57) went on to derive the first general rate equation for the enzymatic conversion of a single substrate to a single product. The general mechanism for this simple enzymatic reaction was described as $E + S \underset{k_{-1}}{\overset{k_1}{\rightleftarrows}} ES \overset{k_2}{\rightleftarrows} E + P$ where E = enzyme, S = substrate, ES = enzyme-substrate complex, and P = product. Michaelis and Menten (58) verified Henri's equation with experimental evidence and plotted initial velocities (V_o) as a function of substrate concentration. The resulting rectangular hyperbola was observed to

asymptotically approach a maximum velocity, V_{max}, which Michaelis and Menten associated with the product $k_2 \cdot [E]_o$. The substrate concentration which yielded a rate equal to 1/2 V_{max} is called the Michaelis-Menten constant (K_M) (59).

The Michaelis-Menten model, actually a model developed by Brown, Henri, Michaelis, and Menten, is a simplified model for a simple enzymatic system and is subject to the following restrictions (59):

1. A single enzyme converts a single substrate to a single product.
2. Only initial rates are measured.
3. The initial concentration of substrate greatly exceeds the concentration of enzyme active sites.
4. Rapid equilibria.
5. The breakdown of the enzyme substrate complex to form product is essentially irreversible.

The requirement for equilibrium is actually a special case of the steady state model described by Briggs and Haldene in 1925 (59). For this model they assumed that the enzyme substrate complex would rapidly reach a steady state concentration. The general form of the equation is the same as the Michaelis-Menten equation with the exception that $K_M = (K_{-1} + K_2)/K_1$, whereas K_M for the Michaelis-Menten equilibrium model is the dissociation constant for the enzyme substrate complex.

The simple model described by Michaelis-Menten kinetics is actually a model of a rare enzyme system since most enzymes catalyze reactions with two or more intermediate interacting substrates (60) and involve several intermediate steps. Nevertheless, the Michaelis-Menten parameters (K_M and V_{max}) are useful in describing enzyme systems (59). Values for K_M and V_{max} can be determined for a complicated system by a univariate method, i.e., by holding the concentration of all substrates constant, usually at a saturating level, and measuring K_M and V_{max} for the substrate whose concentration is permitted to change (60).

Most double substrate reactions can be classified as single-displacement reactions (ordered or random) or double displacement reactions (60,61). With ordered single displacement reactions substrate A must combine first with the enzyme before substrate B combines as shown below:

$$A + E \longleftrightarrow EA$$

$$B + EA \longleftrightarrow EAB$$

The complex EAB may form products and enzyme. In a random single displacement reaction substrate A or B may combine with the enzyme. Creatine kinase is an example of an enzyme which catalyzes a reaction according to the random single displacement model (60).

In single displacement reactions products are formed as the final step of the reaction as opposed to double displacement reactions (60) in which products are formed in different steps of the reaction as shown

$$A + E \longleftrightarrow EA \longleftrightarrow P + E_*$$

$$B + E_* \longleftrightarrow E_* \longleftrightarrow Q + E$$

Where E_* represents a chemically modified form of the enzyme.

Attempts to understand the mechanisms of enzyme catalyzed reactions showing complicated kinetics led to methods for deriving rate equations (62,63). As pointed out above, many enzyme systems do not obey the restrictive assumptions made in the derivation of the Michaelis-Menten equation. The kinetics of these systems are often complicated by multiple steps and intermediates, leading to a steady state rate equation with several kinetic constants (59,61). For example, a transaminase-type reaction such as one catalyzed by hexokinase may have the following general mechanism (59).

$$C_1 + E \underset{k_{-1}}{\overset{k_1}{\longleftrightarrow}} X_1 \underset{k_{-2}}{\overset{k_2}{\longleftrightarrow}} \cdots \underset{k_{-\alpha}}{\overset{k_\alpha}{\longleftrightarrow}} X_\alpha \xleftarrow[k_{-(\alpha+1)}]{k_{\alpha+1}} \cdots \underset{k_{-(f-1)}}{\overset{k_{f-1}}{\longleftrightarrow}} X_{f-1} \underset{k_{-f}}{\overset{k_f}{\longleftrightarrow}} X_f + P_1$$

$$X_f \underset{k_{-(f+1)}}{\overset{k_{f+1}}{\longleftrightarrow}} \cdots \underset{k_{-\beta}}{\overset{k_\beta}{\longleftrightarrow}} X_\beta \xleftarrow[k_{-(\beta+1)}]{k_{\beta+1}} \cdots \underset{k_{-(g+1)}}{\overset{k_{g-1}}{\longleftrightarrow}} X_{g-1}$$

$$C_2 + X_{g-1} \underset{k_{-g}}{\overset{k_g}{\longleftrightarrow}} X_g \xleftarrow[k_{-(g+1)}]{k_{g+1}} \cdots \underset{k_{-\gamma}}{\overset{k_\gamma}{\longleftrightarrow}} X_\gamma \xleftarrow[k_{-(\gamma+1)}]{k_{\gamma+1}} \cdots \underset{k_{-n}}{\overset{k_n}{\longleftrightarrow}} X_n \xleftarrow[k_{-(n+1)}]{k_{n+1}} E + P_2$$

Where C_1 and C_2 are substrates, P_1 and P_2 are products and X_α, X_β and X_γ are isomeric forms of the enzyme complexed intermediates, X_1, X_f and X_g respectively, The steady state rate equation for the general reaction may be derived (59)

$$V = \frac{(V_f/K_f)C_1C_2 - (V_r/K_r)P_1P_2}{(C_1/K_1 + C_2/K_2 + P_1/K_3 + P_2/K_4 + C_1C_2/K_f + P_1P_2/K_r + C_1P_1/K_5 + C_2P_2/K_6 + C_2P_1/K_7 + C_1C_2P_1/K_8 + C_2P_1P_2/K_9)}$$

where the K values are measurable kinetic constants and represent combinations of the rate constants and V_f and V_r represents the maximum forward and reverse reaction rates.

The complicated nature of enzyme kinetics has led to systematic methods for deriving rate equations (62,63). Using these techniques researchers have derived rate equations for many enzyme catalyzed reactions (50,64). The elucidation of enzyme mechanisms continues to be a significant effort with information gained being especially important to physiologists (65).

Coenzymes

Some enzymes require association with a nonprotein molecule in order to perform their catalytic function. If the second species is an organic molecule it is called a coenzyme, e.g., nicotinamide-adenine dinucleotide (NAD), otherwise it is called a cofactor, e.g., Zn^{2+} (60). Coenzymes may be loosely bound to the enzyme and act as a substrate or they may form a tightly bound prosthetic group with the enzyme.

The reactions studied in this research each produce or consume an indicator species as the result of redox reaction catalyzed by an enzyme requiring a coenzyme. Enzymes which catalyze electron transferring (redox) reactions include (60):

1. Pyridine linked dehydrogenases which require NAD or NADP.
2. Flavin-linked dehydrogenases and oxidases which contain flavin dinucleotide (FAD) or flavin mononucleotide (FMN) as a prosthetic group.
3. Iron-sulfur proteins.
4. Cytochromes containing iron-porphyrin prosthetic group.

NAD and NADP are loosely held by dehydrogenases and are regarded as substrates. The kinetics of the reaction follows an ordered bi-substrate reaction in which NAD or NADP is the leading substrate and must bind to the enzyme first. Dehydrogenation occurs by removing hydride from the substrate and transferring it to the C-4 position on the pyridine ring of the coenzyme (66) as shown in Figure 1.

Glucose oxidase is a flavin-linked oxidase and requires FAD as a prosthetic group. Unlike NAD and NADP, flavins are reoxidized by molecular oxygen to yield H_2O_2. They are also easily reoxidized by

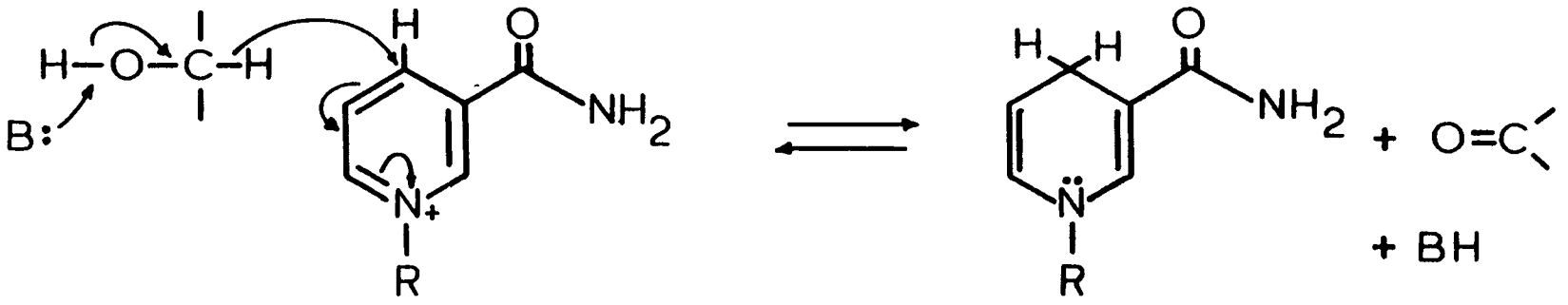

NAD NADH

Figure 1
Two electron reduction of NAD moiety.

artificial electron acceptors such as ferricyanide, methylene blue, phenazine methosulfonate, 2,6 dichlorophenolindophenol; compounds which undergo changes in their absorption spectra upon reduction hence making them useful for spectrometric assays of flavin linked oxidases (60). The isoalloxazine ring of the riboflavin moiety shown in Figure 2 is the active site of electron transfer on the flavin (67). Reduction of the flavin is thought to occur by electron transfer from a carbanion intermediate (67).

Amperometric Oxygen Sensors

The reduction of molecular O_2 at an electrode was observed by Danneel in 1897 (10). Danneel also reported that the electrical current resulting from the reaction was proportional to the concentration of dissolved O_2. Baumberger (68) used a DME at a fixed potential in 1940 to measure O_2 tension, pO_2, in blood and in 1942 Davies and Brink (69) introduced microelectrodes which could be used for measuring local oxygen tension in animal tissues. The microelectrodes constructed were of two types; an open type in which the platinum electrode was directly exposed to the tissue and a closed type in which the end of the platinum wire is recessed inside a small cylindrical glass tip. The open type proved to have a faster response while the recessed type, although slower, enjoyed freedom from convection in the external solution and hence was more stable.

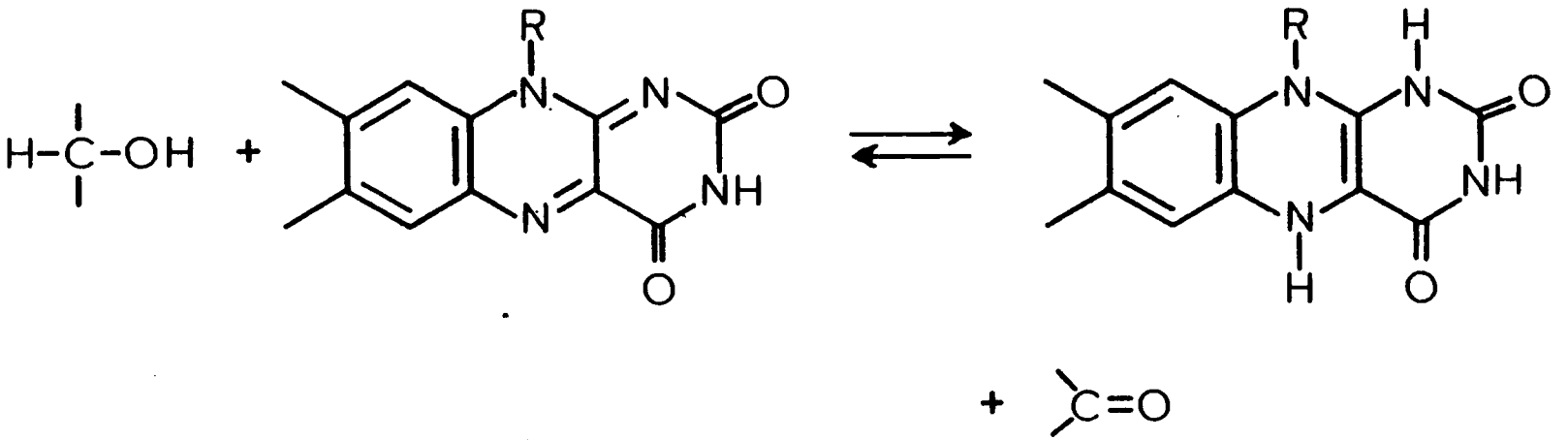

Figure 2
Oxidation and reduction of flavin moiety.

Measurements of O_2 tension, concentration, in tissue were frustrated by the gradual poisoning and resulting loss in sensitivity of the metal cathode by organic species (10). In addition, motion near the cathode surface, resulting in variations in the rate of mass transfer, could not be adequately controlled and the current signal was unstable. A number of attempts were made to either break or control the diffusion layer. These included rotating and vibrating cathodes, coating the cathode with agar, collodion, or cellophane or by recessing the cathode and pulsing the potential (10). Individual semipermeable membranes were used to cover the cathode and the anode, creating a more uniform diffusion layer and partially restricting the passage of organic species. In 1956 Clark (70) reported an electrode design in which the cathode and anode were covered by a single membrane. Since the membrane did not lie in the path of electrical conduction, an oxygen permeable membrane could be used which was impermeable to ions and fully restricted the passage of organic species.

Since their conception, Clark electrodes have enjoyed extensive use as an amperometric method for measuring O_2 tension in tissues, serum, gases and liquids. The characteristics of the Clark electrode, i.e., current output, depends primarily upon the O_2 permeability of impedance layers around the membrane and the geometry of the cathode (71).

Electrode design requires that O_2 pass through three impedance layers; the outer diffusion boundary layer, the membrane and the inner electrolyte layer (10). Stable measurements can be made by making the membrane layer impedance largest, i.e., low permeability, since the other two impedances are likely to change during operation. A low permeability membrane, however, increases the response time of the electrode as given by $t_{99} = 0.53\ Z_m^2/D_m$ (72) where Z_m is membrane thickness and D_m is the diffusion coefficient of O_2. Therefore a compromise must be struck between sensor response time and stability. Response time is also increased with increased cathode area according to the Cottrell equation (73) and is greatest for changes from high to low pO_2 than for the other direction (74).

The lowest concentration of O_2 which can be measured by a given sensor is usually given by $C_{Lim} = I_R/\phi$ where I_R is the residual current and ϕ is the sensitivity of the sensor. Sensor sensitivity, i.e., current output per O_2 concentration is a function of cathode area (71) and membrane permeability to O_2 (75). A highly permeable membrane, therefore, results in increased sensitivity, improved detection limits, and faster response times while less permeable membranes permit more stable measurements and reduce the stirring requirements since the diffusion layer impedance is small compared to the membrane layer impedance. The effect of temperature on current output is quite significant with c.a. 3-4% change in current

output per 1° C (76). The temperature coefficient is greatest for the least permeable membrane.

Membranes are permeable to and cathodes can be poisoned by halogen gases, SO_2, oxides of nitrogen and H_2S (77). However, gold and platinum cathodes are not seriously affected by SO_2 and Cl_2 at concentrations typically encountered in test solutions. Poisoning of platinum cathodes by H_2S does occur readily at potentials more negative than -0.5 V and occurs by blocking the surface sites on the platinum by sulfide (78). Some commercially available sensors are made with a gold cathode (75) and can be used for measuring O_2 in environments containing high concentrations of H_2S.

Immobilized enzyme electrodes have been constructed which utilize an oxygen amperometric detector (5,79-82). A major advantage of these electrodes is the selectivity determined by the enzyme. Enzymes which catalyze reactions utilizing oxygen are immobilized onto a membrane surface and sandwiched between the sensor membrane and an outer dialysis membrane. Under normal conditions, the concentration of O_2 in solution decreases by a rate proportional to the concentration of the analyte species. A change in sensor current is measured and related to the analyte concentration. A new type of enzyme electrode for determining glucose concentrations bonds glucose oxidase with bovine serum albumin directly to the platinum electrode surface (81). Linear calibration graphs over 4 orders of magnitude are reported.

II. EXPERIMENTAL

Computer

Hardware

An Apple II microcomputer was used in all theoretical calculations, data plotting and data acquisition. The Apple microcomputer is based on a 6502 microprocessor (CPU) and is easily programmed in BASIC and machine code. With the disk operating system (DOS) and the Applesoft BASIC interpreter loaded in memory, 13824 memory locations are available to the user for programming and data storage as shown in Figure 3. This amount of memory proved to be sufficient for all applications.

The Apple microcomputer was designed for memory mapped input-output (I/O) meaning that each peripherial device, including the keyboard, is assigned an area of computer memory. Each peripherial device is interfaced through one of eight slots on the back of the Apple microcomputer. Two slots, zero and seven are reserved for special purposes and slots 1-6 may be used for interfacing instruments, printers, plotters, disk drives, etc., to the computer. Each slot has been allocated 280 bytes of memory of which 256 are reserved for read only memory (ROM) or programmable ROM (PROM). The ROM for each slot begins at memory location $CnOO where n is the slot number and "$" signifies a hexadecimal number. The remaining memory locations are reserved for general I/O purposes

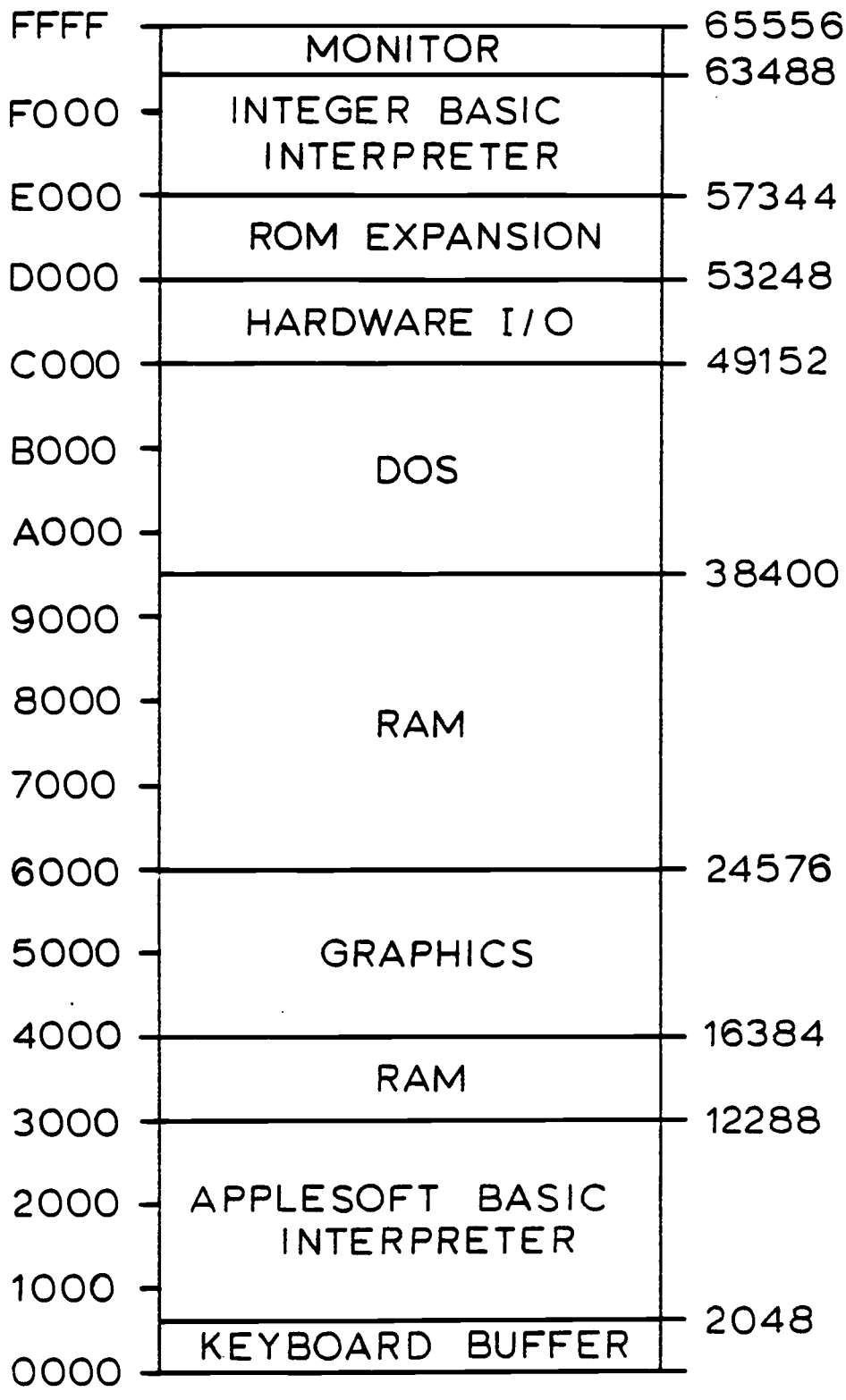

Figure 3
Apple II Memory Map

and start at $COmO where m = n + 8. A peripherial device is selected by reading or writing to a slot which causes the device select line, pin 41, to go low, i.e., less than 1.8 V.

The apple minicomputer sends and receives data in digital form through ports. Data may be transferred serially, i.e., one bit per clock pulse or parallel, i.e., eight bits at a time. A serial port on an RS-232 interface card was used to interface the Apple minicomputer to a printer.

Parallel ports on a Rockwell R6522 versatile interface adapter (VIA) permitted data to be transferred from an analog-to-digital converter (ADC) to computer memory. The 6522 was mounted on an interface card along with additional circuitry to simulate a phase 2 clock by delaying the phase 0 clock signal by 80 ns (83). The card was purchased from John Bell Engineering of Palo Alto, CA. The 6522 is a 40 pin chip and houses 16 internal 8 bit registers.

Figure 4 shows a block diagram of the computer and associated instrumentation and hardware.

Overview of Software

A flexible program (see Appendix II) was written for acquiring data from a variety of instruments. Due to the ease with which one can write BASIC programs, the main body of the program was written

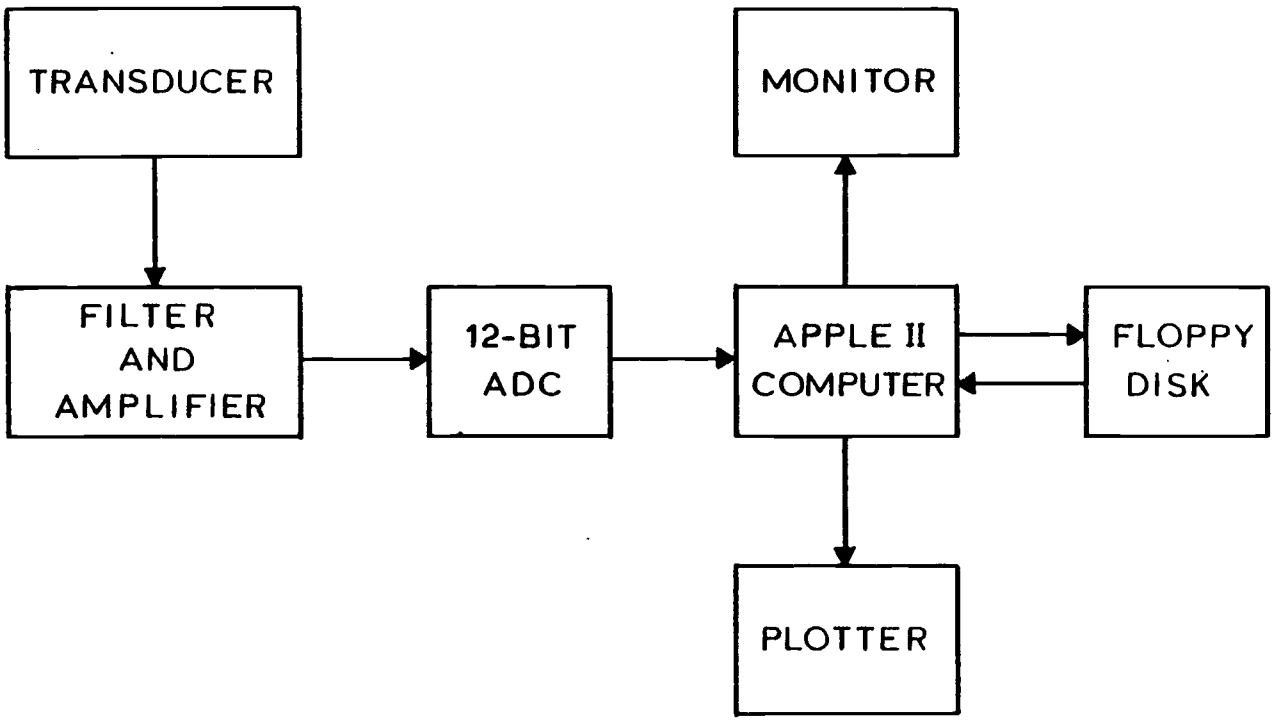

Figure 4
Block diagram of instrumentation and computer

in this language. Machine language subroutines were written to provide a continuous record of elapsed time and sampling the ADC. Some characteristics of the program include: a user controlled variable data acquisition period from 80 ms to 2500 ms per data point, correction for blank signal, display of response curve, calculation of maximum, minimum or inflection point, automatic transfer of data to disk storage at the completion of each run, calculation of the difference integral, and a hard copy of all pertinent data.

After addition of sample to a solution, a few seconds were allowed for mixing prior to the initiation of data acquisition. In order to assure reproducible mixing times for samples and to free the experimenter from computer details at the time of sample introduction, a delay or "lag time" was introduced into the program. After the value for the lag time, e.g., 20 s was input by the user and the return key depressed, the computer started counting down and displaying the elapsed time. At the completion of the countdown the program automatically initiated data acquisition. By observing the countdown on the monitor screen, the experimenter may coordinate the addition of sample with the initiation of data acquisition.

Specific memory locations are allocated to contain the elapsed time and value from the ADC conversion. The machine language subroutines write to these locations and the BASIC program reads them with a "PEEK" statement. The conversion rate is controlled with a loop in the BASIC program in which the elapsed time is continually

read. Each increase in elapsed time of one data acquisition period unit signals the ADC subroutine to be called and the values for the conversion are stored in an array.

The program asks the user to input the data acquisition rate in ms and the total run time in minutes. The number of data points to be collected is then calculated and sufficient memory is set aside to store the data points in an array by the use of a dimension statement (DIM). An array is a table of values with i columns and j rows for a particular variable Y. For example Y(i,j) is the value of Y in the i^{th} row and the j^{th} column. Even though each array element requires 5 bytes of memory, data were stored in this fashion as opposed to specific memory locations since transfer of the data to and from disk is much easier and permits greater flexibility in the use of computer memory.

First and second derivatives for each run may be calculated immediately after each run or at the completion of the experiment. Due to the long execution time required for estimating derivatives, this calculation was postponed until the experiment was complete for runs in excess of three minutes. For theoretical calculations the time of the first derivative can easily be found since there is little noise on the curve. For example, the time of the maximum may be found by noting the time at which the largest value for the signal is observed. Analyses of real samples, however, must deal with noise. Therefore a sequence of points suggesting a trend in the

response curve, as opposed to a single point which may be due to noise, are used to determine derivatives. To accomplish this the program first performs a least squares analysis over a small portion of the curve between data points 0 and n where n is the number of data points and is input by the user. The computer saves the calculated slope for this short interval and stores the slope in an array in memory. A least squares analysis is then performed from 0+1 to n+1 and the slope also saved in memory. The process is repeated for all the data points or until a first derivative of zero is encountered, preceeded by several nonzero first derivative estimates.

After three consecutive slopes have been calculated the program compares the values to find the maximum or mimimum. For example, in determining the maximum the program first searches the calculated slopes for the first three consecutive negative values. If the search proves futile, the analysis interval is incremented by one and a new slope is calculated and compared to the previous two. After three consecutive negative slopes have been found a flag is set signifiying to the program that a maximum has been passed and additional searching is unnecessary. The time of the maximum is found by subtracting three from the loop counter and multiplying the result by the time increment for each data point.

The times of the minima were determined in an analogous fashion. Several curves, however, exhibited a minimum plateau instead of a minimum point. Since the minima for these curves were diffuse,

in some cases over several minutes, the time of the minimum could not be easily defined. In order to characterize these curves, the time at which the response fell below a predetermined signal level was used as a substitute for the time of minimum. This threshold signal level was chosen to be only slightly higher than the plateau.

Inflection points were determined by a method of Savitzky and Golay (87). With this method second derivatives are estimated at all points along the curve by convoluting the data points with an appropriate set of integers given by Savitzky and Golay (87). The inflection point is determined from the second derivative nearest zero.

Technical Discussion of Software

Input analog signals are continually converted to digital numbers by the ADC. Since the conversion rate of the ADC is about 25 μs, the computer would quickly run out of memory if each datum was collected. In addition, it would be unnecessary to sample the ADC at such a high frequency since a lower sampling rate would yield the same results for these experiments. Therefore, a subroutine was written to signal the microcomputer when it was time to sample the ADC output. The computer diverts from the main program to this subroutine when it encounters the statement "call 38240" (see Appendix II for a listing of the machine language subroutine). 38240 is the

decimal location for the machine language subroutine located at $9560.

The first part of the subroutine loads the auxiliary control register (ACR) of the 6522 with the number $40, thus setting bit number 6 of the ACR. This sets the T1 timer to operate in the free run mode. The next few lines load the low byte of the T1 timer latch ($C104) with the number 14 ($0E) and the counter high byte ($C105) with 39 ($27). Writing to T1 counter high loads the value in the T1 latch into the T1 counter low byte and starts the T1 timer countdown.

The total count in the T1 timer is 39*256 + 14 = 9998. Two additional clock cycles are required to load the values contained in the high and low latches into the counter at the start of each T1 countdown. The total number of clock cycles per countdown, therefore, is 10000. The T1 timer begins to countdown at the rate of 1 count per cycle (1 μs). At the end of 10000 clock cycles (10 ms) the timer will set an interrupt flag, reload the high and low bytes of the T1 timer and countdown again. Thus an interrupt flag is set every 10 ms. The memory locations which keep record of the number of T1 countdowns, $9583 and $9584 are initialized by loading zero in each location. Memory location $9585 stores the sampling rate in centiseconds and is loaded from the BASIC program by "POKING" the value into 38264 ($9578).

The last register to be addressed is the interrupt enable register (IER) at $C10E. By loading the IER with $C0, bits 6 and 7 are set thus enabling the CPU to recognize when an interrupt flag has been set by the T1 timer. Since a nonmaskable interrupt is used is not necessary to clear the interrupt disable (CLI). The interrupt flag is reset by reading the low byte of the T1 timer counter thus enabling the T1 timer to set another interrupt flag and cause another interrupt. It can also be reset by writing to the T1 counter high byte. The last command in this portion of the machine code program is return from subroutine (RTS) and returns the Apple microcomputer to the BASIC portion of the program.

After 10 ms the counter values in T1 timer are at zero and an interrupt flag is set causing the CPU to jump to the vector address at $3FB-$3FD. The vector address was previously loaded with the code for jump (JMP) to the memory location $9586. Thus upon receiving an interrupt, the computer executes the machine language program which starts at $9586. The first command of interest pushes the value in the accumulator onto the stack. The stack is located at page 1 of computer memory ($100-$1FF) and is used for temporary storage.

Since the contents of the accumulator would be lost in the next several statements it is necessary to save its present contents so that the computer can resume execution where it left off before the interrupt. The next instruction resets the interrupt flag by read-

ing the T1 timer low byte counter ($C104). This is necessary so that the computer can recognize additional interrupts. Next the interrupt counter ($9585) is decreased (DEC) by one. Since the Apple microcomputer had earlier calculated the number of interrupts required before the ADC can be sampled and had loaded this location with that number, it is now waiting for that number to go to zero.

The next statement checks the value in $9585 to see if it is zero. If it is not zero the program branches to $959E. If it is zero the original number of interrupts is reloaded into $9585 and $9583 is incremented (INC) by one. Since 255 ($FF) is the largest number each memory location can contain, $9583 is checked to see if it has been incremented beyond that value; if it has, then zero will be stored in $9583 and the CPU will increment $9584 by one. These locations are used to contain the high and low bytes of the elapsed time. The accumulator is now pulled off the stack and the return from interrupt instruction (RTI) returns the computer to the program it left prior to servicing the interrupt.

Most of the time the BASIC program is engaged in examining the time locations at 38275 ($9583) and 38276 ($9584). Since $9584 is the high byte and $9583 the low, the current time is determined by multiplying $9584 by 256 and adding the product to the contents of $9583. The sum is then multiplied by the sampling rate in seconds to compute the present time. This number is then compared with the value computed the last time the CPU polled these locations. If the

values are the same, the CPU continues to poll, if the new value has increased, it signifies to the computer that it is time to sample the ADC.

The computer execution then branches to line 120 where the command "CALL 38305" causes execution to begin at the machine language subroutine starting at $95A1. This subroutine will sample the ADC once. The data direction registers (DDR) for Ports A and B on the 6522 VIA are initially configured to make port A ($C101) an output port and port B an input. This is accomplished by writing all "1"'s ($FF) into DDRA ($C103) and all "0"'s into DDRB (C102). Next the peripheral control register (PRC) is configured so that it may recognize when the ADC has completed a conversion. The number $E0 is placed in the PCR. This clears bit 4 which causes the CB1 interrupt flag to be set on a negative transition. In addition, CB2 is set in the high mode.

The next instruction loads the PCR with the number $C0, making CB2 low. The CB2 level is raised and the conversion started by placing $E0 in the PCR. When the ADC has finished a conversion, CB1 will go low and the CB1 interrupt flag in the interrupt flag register (IFR) will be set. The CPU polls the interrupt flag register, IFR ($C10D) by bit testing it with the number $10. The bit test performs a "logical AND" with the accumulator contents. Since the CB1 flag is bit 4 in the IFR, the IFR contains the number $10, binary 1000, when CB1 goes low and the bit test reports nonzero.

This result causes program execution to branch out of the polling loop and sample the input port ($C100) containing the high byte of the conversion. The contents of the input port are placed in the Y register. Since the ADC used is a 12-bit converter and the Apple microcomputer has only an 8 bit data bus, the ADC had to be read twice, once for the upper 8 bits (high byte) and again for the lower 4 bits (low byte). After reading the upper 8 bits, the number $09 is placed on the output port ($C101) to set the mode so the ADC will send the lower byte. The low byte is read at the input port ($C100) and stored in the accumulator. The low and high bytes are transferred to memory locations $95D9 and $95D8 respectively. Program execution then resumes at the BASIC portion of the program and the high and low bytes are combined and stored in an array.

Initially a normal interrupt request (IRQ) was used for signaling a T1 countdown. A nonmaskable interrupt (NMI), however, is used instead since program execution will not resume when returning from the machine language subroutine to basic after being interrupted by IRQ. The interrupt enable register (IER) on the 6522 is disabled prior to transferring data to the disk drive to avoid a similar problem. This is accomplished by a machine language subroutine at 38364 ($95DC). After the data are transferred, the IER is enabled by the subroutine at 38268 ($957C).

Programs for Theoretical Calculations

The first phase of this research evaluated the validity of difference integral calculations for response curves exhibiting maxima, minima or inflections. Response curves representing idealized kinetic models were generated by a computer program using published theoretical rate equations and data (50-53). Each response curve was generated from a computer program which calculated the time dependent concentrations of reaction species and the response expected for a given indicator species concentration (see Appendix II).

Calculations are based on an iterative routine which approximates concentration of the time dependent indicator species, [I] from the calculated rate over a small time interval, Δt. At the start of each program the initial concentrations of each reactant are input along with the time of each iteration, Δt, and the run time. The program then approximates the derivative, $d[I]/dt$, based upon the initial concentrations, and multiplies the rate by Δt to obtain $\Delta[I]$. Each reactant concentration is then diminished an amount $\Delta[I]$ and the product concentrations are increased by $\Delta[I]$. The concentration of the indicator species is stored in an array in memory and the iteration repeated for a second Δt using the "new" concentrations for the reactants and products in the rate equation. The process continues until the sum of the Δt values

equals the total run time. Values for the signal response for each Δt increment are calculated from the indicator species concentration using an appropriate relation and stored in an array in computer memory.

The calculated signal response values are integrated using Simpson's rule (84) and the value of the integral is stored in memory. The maximum point is found by examining each calculated indicator species concentration or response and noting the time for the largest value. The minimum is found by noting the time of the smallest response.

At the completion of these calculations the response vs. time curve is displayed on the monitor screen and the integral and time of the maxima, minima or inflection point are printed on hard copy. The concentrations are restored to their initial values and the iterative routine repeated. For an enzyme assay the enzyme concentration is incremented an amount Δ[enzyme] and the new enzyme concentration used in the next calculation. For a substrate determination the substrate concentration in incremented an amount Δ[substrate] the calculations are then repeated at the new analyte concentration and a second integral is calculated. This process continues until a specified number of integrals are obtained. Integral data are then transferred to a text file on disk and difference

integrals are plotted as a function of enzyme activity or substrate concentration.

Theoretical Response Curves Exhibiting Maxima

Response vs. time curves exhibiting maxima were generated from published kinetic data (50) to model lactate dehydrogenase (LDH) assays. LDH catalyzes the oxidation of lactate in an ordered single displacement reaction. The overall reaction of the multistep reversible oxidation may be represented as, lactate + NAD$\leftrightarrow$pyruvate + NADH with NAD acting as a second substrate. A computer program calculated the reaction rates from the equation

$$\frac{d[P]}{dt} = \frac{(V_{ab}/K_{ab})([A][B]) - (V_{pq}/K_{pq})([P][Q])}{1+\frac{[A]}{K_a}+\frac{[B]}{K_b}+\frac{[P]}{K_p}+\frac{[Q]}{K_q}+\frac{[A][B]}{K_{ab}}+\frac{[P][Q]}{K_{pq}}+\frac{[A][P]}{K_{ap}}+\frac{[B][Q]}{K_{bq}}} \quad (1)$$

where V values are maximum velocities of the reaction in the forward and reverse direction and include LDH concentration, A = lactate, B = NAD, P = pyruvate, and Q = NADH, the indicator species. The K values represent aggregates of the individual rate constants and are determined from initial rate data. For example, K_a is calculated from the Michaelis-Menton constant for the reaction when [B] is maintained at a high, saturating level and the initial concentrations of products are negligible. K_{ap} is determined from the Michaelis-Menton constant for the reaction when [B] and [P] are high

and the initial concentration of a is negligible. Alberty et al., (50) have also derived relationships among the constants for calculating additional constants.

The fluoresence signal was then calculated from the relation

$$(E_f)_t = K \; 10^{-\varepsilon b_1 [Q]_t} \; 1\text{-}10^{-\varepsilon \Delta b [Q]_t} \; 10^{-\varepsilon b [Q]_t / 2} \qquad (2)$$

where ε' = molar absorptivity at emission wavelength, ε = molar absorptivity at excitation wavelength, the b values are cell path-length parameters, and K is a collection of variables independent of analyte concentration (85). The first parenthetical expression equates absorbance of radiation due to inner filter effects and the last expression in parentheses accounts for absorbance of emission radiation due to post-filter effects. Values for the variables shown in equation 2 were modified to afford sufficient pre- and post-filter effects over the concentration range studied. Thus ε = 10000 L mol^{-1} cm^{-1}, ε' = 50000 L mol^{-1} cm^{-1}, K = 100, and the b values were 2 mm each.

The program calculated time dependent concentrations of each species at each iteration, Δt, by approximating Δ[NADH] and adding Δ[NADH] to $[\text{pyruvate}]_t$ and $[\text{NADH}]_t$ and subtracting Δ[NADH] from $[\text{lactate}]_t$ and $[\text{NAD}]_t$. $[\text{NADH}]_t$ was used in equation 2 to calculate the theoretical fluorescence response at each iteration. The time

of the maximum fluorescence response was determined by multiplying the value in the loop counter of the iteration resulting in a maximum value for E_f by the theoretical acquisition rate. Values for the time dependent fluorescence response and the time corresponding to the maximum response were stored in an array in computer memory. At the completion of each run the fluorescence response was numerically integrated over time and the value of the integral stored in an array. After a specified number of curves had been integrated, the integral data were plotted on the monitor screen as a function of $[LDH]_0$ and the data transferred to disk memory.

Theoretical Response Curves Exhibing Minima

Response *vs.* time curves exhibiting minima were generated from published kinetic data (51) to model glucose determinations. Glucose oxidase catalyzes the oxidation of glucose according to the overall reaction, glucose + O_2 + H_2O ⟶ gluconic acid + H_2O_2. The rate of oxidation of glucose may be determined by monitoring the time dependent concentration of O_2. Depletion of O_2 by the enzymatic reaction occurs at a rate given by (51)

$$-d([O_2]/dt)_E = [E]_t(1/k_1[G] + 1/k_2 + 1/k_3[O_2] + 1/k_4)^{-1} \qquad (3)$$

where the k values are kinetic constants, [G] = glucose concentration, $[O_2]$ = O_2 concentration, $[E]_t$ = concentration of glucose oxidase at time t and the subscript E indicates a rate of depletion of O_2 by the enzymatic reaction.

The concentration of O_2 is also affected by the rate at which O_2 diffuses into the solution from the surrounding environment. The rate of diffusion of O_2 into the system is given by (86)

$$(d[O_2]/dt)_D = K(([O_2]_{eq} - [O_2]_t)/[O_2]_{eq}) \quad (4)$$

where K is an empirically determined constant (86), $[O]_{eq}$ is the oxygen concentration when the solution is equilibrated with air and the subscript D indicates a rate of diffusion of O_2 from the surrounding environment into the solution.

If we neglect nonenzymatic factors then the overall rate of change of oxygen is given by (86)

$$d([O_2]/dt) = (d[O_2]/dt)_E + (d[O_2]/dt)_D \quad (5)$$

A program was written (see Appendix II) to calculate the time dependent concentration of O_2, $[O_2]_t$, over the integration interval. Input statements interrupt program execution and ask the user for initial glucose concentration, Δt for each iteration, total run time and amount to increment glucose for each run. Program execution resumes after inputting the required data. Constants used

in the equations were obtained from the literature (51). The constants and the initial i.e., equilibrium concentration, of O_2 are loaded from the program.

Time dependent concentrations of O_2 were calculated by estimating $\Delta[O_2]$ over the small time interval, Δt, using equations 3-5 and summing $\Delta[O_2]$ over the integration interval.

The incremental change in $[O_2]$ due to the enzymatic reaction, $\Delta[O_2]_E$, was estimated from the rate given in equation 3 where $\Delta[O_2]_E = (d[O_2]/dt)_E \cdot \Delta t$. The incremental change in $[O_2]$ due to diffusion was calculated from equation 4 where $\Delta[O_2]_D = (d[O_2]/dt)_D \cdot \Delta t$ and the total change in $[O_2]$ for the iteration was calculated from equation 5. One to one stoichiometry in the reaction requires the [glucose] to decrease an amount $\Delta[O_2]_E$ at the completion of each iteration. The total concentration of O_2 is determined from $[O_2] = [O_2]_{eq} + \sum_{j=1}^{n} \Delta[O_2]$ and the concentration of glucose is given by $[G] = [G]_i + \sum_{j=1}^{n} \Delta[O_2]_E$ where j is the present number of iterations and i signifies initial concentrations.

Values of $[O_2]_t$ at each iteration were stored in an array in computer memory and at the completion of the run $[O_2]_t$ was numerically integrated over time. The difference integral was calculated by subtracting the integral of $[O_2]_t$ from the integral of $[O_2]_{eq}$ over the integration iterval. The time corresponding to the minimum $[O_2]_t$ was also determined by storing the loop counter corresponding

to the minimum $[O_2]_t$ in memory and multiplying the value in the loop counter by the theoretical data acquisition rate. The concentration of glucose was incremented by an amount input at the start of the program and the iterative calculations repeated at the new glucose concentration. All calculated values were stored in an array in the computer memory. Values for $[O_2]_t$ were transferred to disk storage as text files; the number of arrays transferred and which ones to be transferred were determined at the beginning of the program by the user. After a specified number of curves had been integrated, the difference integrals were recalled and plotted on the monitor screen as a function of initial glucose concentration. A printout of initial glucose concentration, $[G]_i$, value of the difference integral and time of the minimum completed the program execution. A similar program was written for modeling glucose oxidase assays in which the initial concentration of glucose was held constant and the enzyme concentration was allowed to change.

Theoretical Response Curves Exhibiting Inflection Points

Theoretical response curves modeling creatine phosphokinase (CPK) assays and exhibiting points of inflection were generated from published kinetic data (50, 52, 53) using three equations in a consecutive coupled reaction. The overall reaction is represented by

$$\text{ADP} + \text{Creatine Phosphate} \xleftrightarrow{\text{CPK}} \text{Creatine} + \text{ATP}$$

$$\text{ATP} + \text{Glucose} \xleftrightarrow{\text{HK}} \text{G6P} + \text{ADP}$$

$$\text{G6P} + \text{NADP} \xleftrightarrow{\text{G6PD}} \text{6-Phosphogluconate} + \text{NADH}$$

The first step is catalyzed by CPK, the second by hexokinase (HK) and the third by glucose-6-phosphate dehydrogenase (G6PD). The rate of the first reaction determines the rate at which ATP is produced and was calculated from the relation (53),

$$\frac{d[D]}{dt} = \frac{V_1[A][B] - V_2[P][Q]K_{ia}K_b/K_pK_q}{K_{ia}K_b + K_b[A] + K_a[B] + [AB] + \frac{K_{ia}K_b[A][P]}{K_{ip}K_{Ia}} + \frac{K_{ia}K_b[P]}{K_{ip}} + \frac{K_{ia}K_b[Q]}{K_{iq}} + \frac{K_{ia}K_b[P][Q]}{K_pK_{iq}} + \frac{K_{ia}K_b[B]}{K_{iq}K_{Ib}}} \quad (6)$$

V_1 and V_2 represent the maximum velocities of the reaction in the forward and reverse directions, respectively, and A = ADP, B = Phosphocreatine, C = Creatine, and D = ATP. The constants symbolized by K_n where n = a, b, p, or q are Michaelis-Menten Constants and K_{in} and K_{In} represent enzyme complex dissociation constants.

The rate of the second step determines the rate at which ATP is consumed by the first reaction and also the rate at which G6P is produced. The rate was computed from the relation (52),

$$\frac{d[ATP]}{dt} = \frac{[E]_o}{k_1 + k_2/[G] + k_3/[ATP] + k_4/[G][ATP]} \quad (7)$$

where the K values are kinetic constants, $[E]_o$ = initial concentration of hexokinase and, [G] = glucose concentration.

The rate at which the indicator species, NADPH, is generated is determined from the final step to the reaction using equation 1 where A = G6P, B = NADP, P = 6-phosphogluconate and Q = NADPH. Kinetic parameters for LDH were used to estimate the reaction catalyzed by G6PD since the reactions are similar (59).

The program calculates the rate for each step of the reaction from the above equations at each iteration of Δt. The concentrations of species which link steps, e.g., ATP and G6P, were determined by subtracting the rate at which the species was consumed in one step from the rate at which it was produced in a second step and multiplying the result by Δt and summing the incremental concentrations over the iteration period. Concentrations of species which were not linked were calculated by approximating changes in concentrations during incremental time intervals, Δt, and summing the changes over the iterations. The time dependent concentration of the indicator species, NADPH, was calculated and values for $[NADPH]_t$ were numerically integrated and transferred to disk memory. Since the initial concentration of NADPH is zero, the difference integral is equal to the integral of the $[NADPH]_t$ *vs.* time curve. After a specified number of curves had been integrated, the integral data

were transferred to disk storage and plotted as a function of $[CPK]_o$.

Apparatus and Reagents

All reagents were purchased from Sigma Biochemicals Co., St. Louis, MO. Deionized water was used in the preparation of all solutions. Table I shows stock solutions used.

An Oxford autopipet, adjustable from 1 mL to 5 mL was used for rapid delivery of solution volumes within this range. Solutions were drawn slowly to prevent bubble formation inside the autopipet tip. Addition of samples with volumes between 100 µL and 500 µL was accomplished with an Eppendorf pipet with disposable tips. Solution volumes in excess of 5 mL were delivered using glass volumetric pipets.

The reproducibility of each pipetting device was studied. For this study an empty 10 mL beaker was weighed to the nearest 0.1 mg and a known volume of water transferred and weighed using different settings of the adjustable pipet and a glass volumetric pipet.

Detection limits were calculated for each analytical technique using the relation $C_l = \frac{2\sigma b}{m}$ where C_l is the concentration of the analyte at the detection limit, σ_b is the standard deviation of the signal due to blank, and m is the slope of the linear portion of the calibration plot.

Table I
Stock Solutions for Assays

Reagent	Comments
phosphate buffer pH 7.5	0.1 M. Dissolve 0.08 mol (11.4g) Na_2HPO_4 and 0.02 moles (2.76g) $NaH_2PO_4 \cdot H_2O$ in 1.0 L H_2O.
phosphate buffer pH 5.5	0.1 M. Dissolve 14.0 g Na_2HPO_4 and 0.5 g $NaHPO_4$ in 1.0 L H_2O.
pyrophosphate buffer	0.032 M. Dissolve 143 g $Na_4P_2O_7 \cdot 10H_2O$ in 10 L H_2O. Add 42.5% H_3PO_4 dropwise until pH is 8.8.
tris buffer	0.2 M. Dissolve 12.12 g trihydroxymethylaminomethane (trizma base) in 500 mL H_2O and add 6 N HCl dropwise until pH is 7.3. Dilute to 0.05 M as needed.
ethanol	1000 mg/100 mL. Dilute 12.7 mL 100% ethanol to 1.0 L with pyrophosphate buffer.
NAD	Dissolve 250 mg in 8 mL 0.1 M phosphate buffer pH 7.5.
ADH	Dissolve 2 mg lyopholized ADH (325 IU/mg solid) in 1.0 mL phosphate buffer pH 7.5.
glucose	0.0 1M. Dissolve 1.8 g β-D-glucose in 1.0 L phosphase buffer pH 5.5.
glucose oxidase	Dissolve 54.2 mg glucose oxidase (130 U/mg solid) in 10.0 mL 0.1 M phosphate buffer pH 7.5.
CPK	Dissolve 9.4 mg lyphosized CPK (130 U/mg solid) in 5.0 mL 0.05 M tris buffer.
CPK auxiliary reactions	Dissolve the following reagents in 100 mL 0.05 M tris buffer: 286 mg creatine phosphate, 51 mg ADP, 360 mg glucose, 428 mg $MgCl_2 \cdot 6H_2O$, 392 mg AMP, 1.7 mg hexokinase (80 U/mg solid), 29.3 mg NADP, 80 mg cysteine · HCl, 0.5 g glucose-6-phosphate dehydrogenase (220 U/mg solid)

Analytical Instrumentation

Fluorometry

Ethanol analyses were performed with ADH using NADH as the indicator species. The fluorescence of NADH was measured with a Varian SF-330 Spectrofluorometer at the following settings:

Excitation Wavelength:	340 nm
Emission Wavelength:	474 nm
Excitation Bandpass:	10 nm
Emission Bandpass:	10 nm
PMT voltage:	-418 V

Radiation from a 150 watt Xenon arc lamp is dispersed on a concave grating with 1200 lines/mm. The dispersed radiation is passed through an exit slit and chopped by a rotating circular disk. The chopped radiation is passed through a semitransparent quartz plate; some of the radiation being reflected to the reference PMT and the remainder passing through the plate. After passing through the sample cell and emission slit, the radiation is detected by the sample PMT.

The cell compartment of the fluorometer was modified slightly to accommodate a stirring motor as shown in Figure 5. The housing on a small stirring motor was removed and the motor mounted to a small block of wood. The cord to the motor was severed and a small

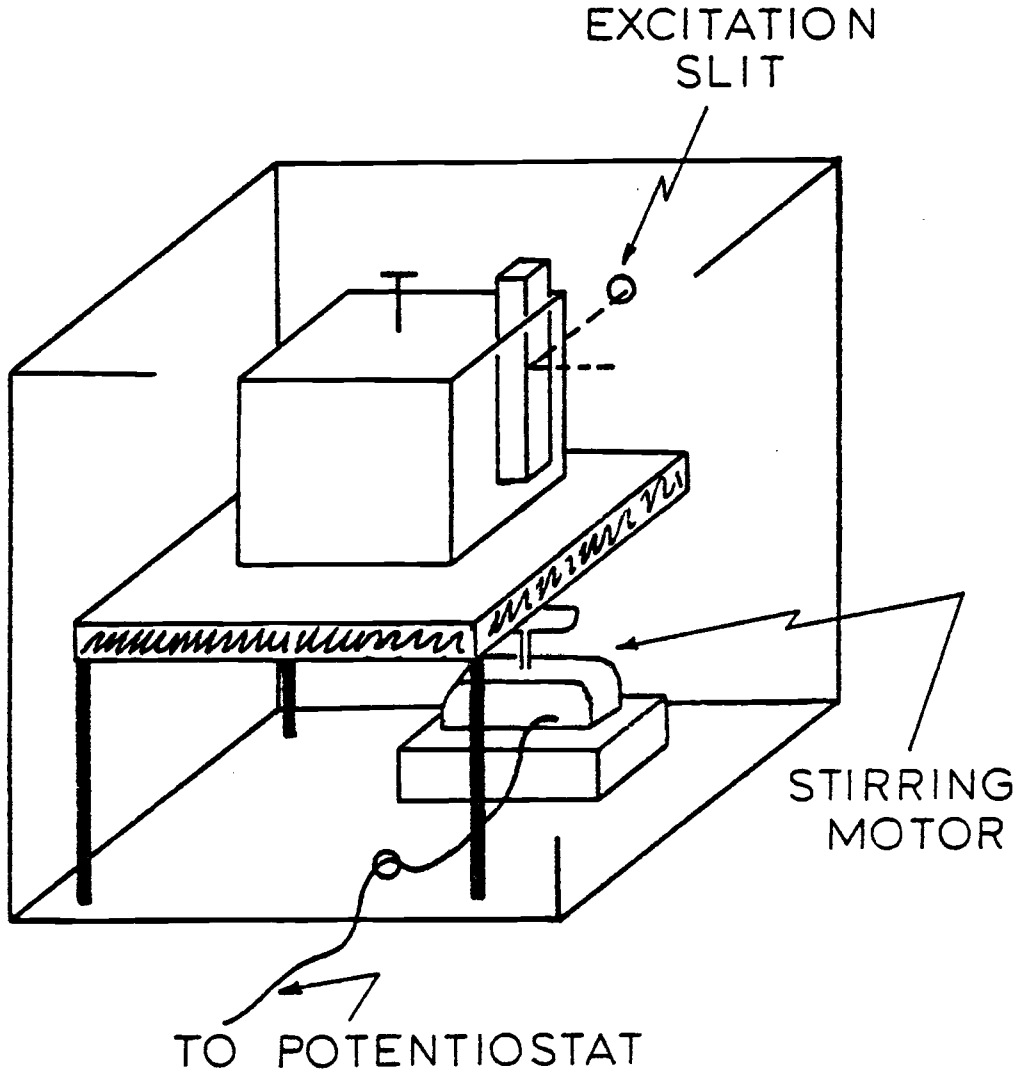

Figure 5
Modification of Fluorometer

in-line plug installed to allow the cord to pass through a 1/4 in. hole. A leg on the carrousel was removed to make room for the stirring motor which was then placed at the base of the carrousel. The cell selector knob and attached shaft and gear were also removed and the cord to the stirring motor passed through the opening. The hole was then sealed with black electrical tape and the cord connected to the motor via the in-line plug. The motor was plugged into a variable powerstat. A small circular stirring bar (1 cm diameter) was placed into the cell and the cell placed in the carrousel. With the cell full of water the potentiostat was turned on and the motor position adjusted slightly to achieve efficient stirring. The potentiostat voltage was then adjusted to achieve an optimal stirring rate. The ADC was connected to the recorder output on the fluorometer.

Amperometry

The amperometry cell used for performing glucose assays was constructed from a 30 mL beaker and a Beckman oxygen sensor (model 0260) as shown in Figure 6. A 6 mm diameter hole was bored into the side of the beaker about 2 cm from the bottom. Through this hole the sensor tip was introduced far enough to permit the membrane to be flush with the interior wall of the beaker. The sensor tip was

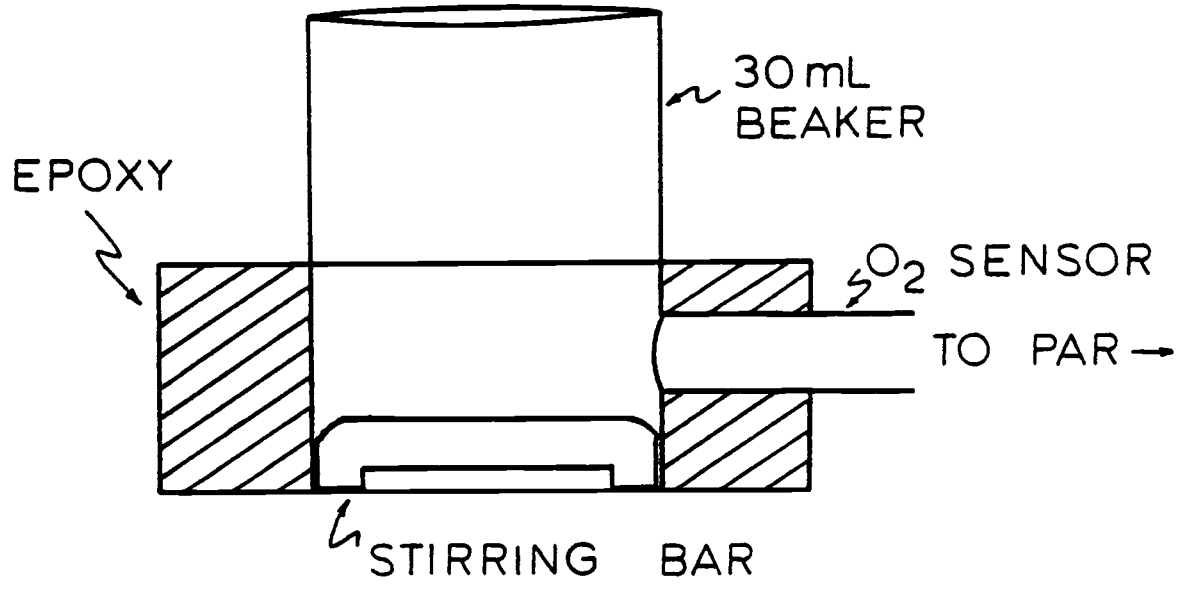

Figure 6
Side view of amperometry cell.

sealed in place with Torrseal and a 1.5 cm thick epoxy base was cast around the bottom half of the beaker for structural support. The sensor was easily inserted and removed from the mounted tip to permit changing the membrane and refilling of electrolyte solution.

The Pt working electrode and the Ag/AgCl reference electrode of the sensor were connected to a Princeton Applied Research Model 174A (PAR) potentiostat and the working electrode was maintained at -0.55 V *vs.* Ag/AgCl. Current output from the sensor was monitored as an output voltage via the Y-axis from the PAR.

The assembly was mounted to a ringstand and positioned about 7 cm above a stirring motor to afford thermal insulation from the motor. A teflon covered circular stirring bar was placed inside the beaker and the stirring rate held constant for each group of assays.

Absorbance

CPK assays were performed using a coupled consecutive reaction and monitoring the absorbance of the indicator species, NADPH, with a Cary 118C Spectrometer. The spectrometer settings used are listed below:

Wavelength:	340 nm
Slit width	1 mm (5 nm bandpass)
Gain	0.3
Absorbance range	0-2

Radiation from the tungsten lamp source was dispersed with a prism using an aluminum coated reflecting back. Incident and reflected radiation were passed through the front face of the prism and the dispersed radiation chopped by a rotating circular disk. The dispersed radiation was passed alternately through the sample and reference cells and on to the PMT.

The cell compartment of the spectrometer was constructed such that simple modification to accommodate a stirring motor was not feasible. Solutions were mixed, therefore, outside of the cell prior to data acquisition. The signal output was monitored by the ADC by attaching a wire to the pen servo mechanism. The voltage of this wire varied from -15 V at zero absorbance (left scale) to +15 V at maximum absorbance (right scale). The scale voltages were too large for the operational amplifier inputs so a voltage divider was constructed from two 20 x 10^6 Ω resistors to reduce the voltage by 50%. The input of the amplifier and filter was connected to the divider and the output voltage of the amplifier adjusted to approximately 10 V for a full scale deflection of the pen. The ADC was used in the bidirectional mode to enable proper scaling over the positive and negative voltages.

Data Handling

The transducer output from the spectrometer and the amperometry cell was monitored through an active filter and a variable

amplifier. The signal from the fluorometer was sufficiently filtered to permit direct connection to the amplifier. The amplifier and filter were constructed from TL-081 operational amplifiers. Figure 7 shows the schematic for the filter and amplifier. The amplifier was configured as a inverting amplifier with a 8200 Ω feedback resistor and a 0 to 2000 Ω variable input trimming resistor. The maximum allowable input voltage to the ADC was 10 V so the trimming potentiometer was adjusted to make the maximum transducer signal input correspond to a 10 V amplifier output. The amplifier output was connected to a 12 bit ADC with a 25 μs conversion time.

The Apple II microcomputer was interfaced to an ADC through parallel ports on a 6522 versatile interface adapter as discussed above. The addressable timers on the VIA were programmed to set interrupts every 10 ms. The data acquisition rate was programmed to be a multiple of the 10 ms interrupt rate and was controlled by selection of the desired rate at the start of the program.

The high resolution graphics mode of the Apple II was used for displaying data on the monitor screen. Text files of the data were created and stored on 5.25" Verbatim floppy disks.

Assays and Analyses

Assays for glucose oxidase and CPK and determinations for ethanol were performed using difference integral calculations. Each response curve was numerically integrated over a fixed time interval

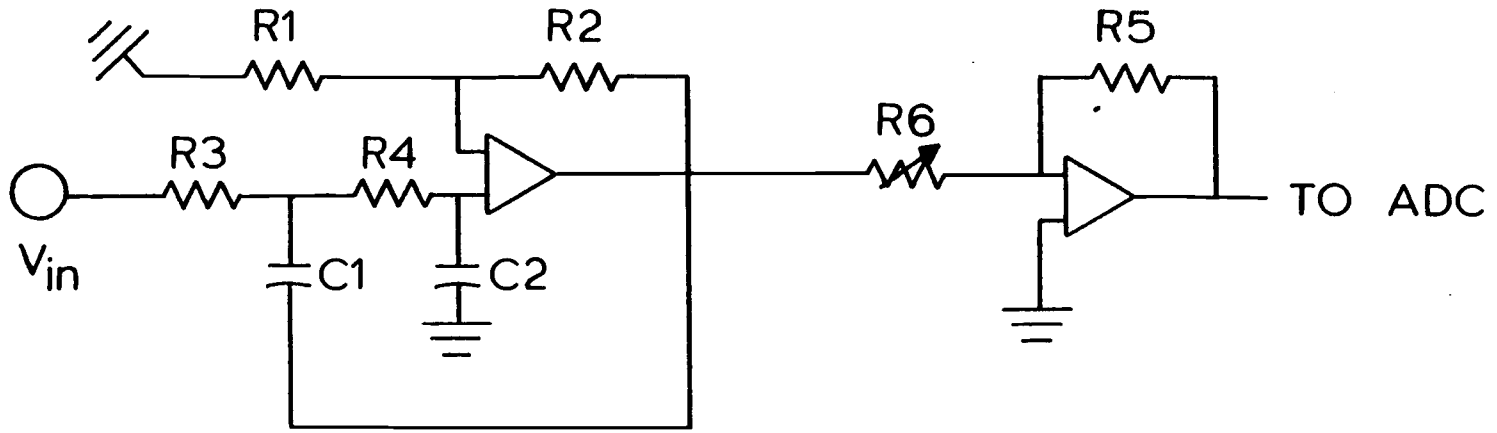

Figure 7
Schematic of active filter and variable amplifier. R1 = 120KΩ, R2 = 1.8KΩ R3 = R4 = 1-KΩ, R6 = 0-2 KΩ, R7 = 8KΩ, C1 = C2 = 0.1 μF.

using the computational programs. The difference integral for glucose oxidase was calculated by subtracting the integral of the time dependent current output from the initial current output. All other difference integrals were equal to the integral of the response curve since the initial concentrations of indicator species, NADH and NADPH, were neglibible in all cases. The program performed sequential least squares analyses over small time intervals of each response curve to estimate the first derivative. Second derivatives were estimated using the method described by Savitzky and Golay (87).

Ethanol Determinations

The fluorometer was modified and electrical connections made as described in the Analytical Instrumentation section. Power to the fluorometer was turned on 2 hours prior to the determinations.

It was desired to have approximately equal numbers of ethanol solutions which did and did not exhibit maxima within a 60 s integration period. Therefore, the ADH activity was adjusted using an ethanol solution of intermediate concentration (100 mg/100 mL). The proper ADH activity was selected by adding ADH dropwise to the NAD solution and observing the response curve resulting from 100)L of the ADH solution in 2.5 mL of 100 mg/100 mL ethanol solution.

Sufficient ADH was added to cause the fluorescence signal to reach a maximum at approximately 60 s.

Determinations were initiated by adding 2.5 mL of an ethanol solution to the cell and turning the stirring motor on. The lag time was 10 s and the run time was set to 2 min. 100 µL of the ADH/NAD solution were added with an autopipet 4 s before initiation of data acquisition. The fluorescence signal was sampled every 500 ms for two minutes and at the end of two minutes the contents of the cell were removed by vacuum suction and the cell was rinsed three times with distilled water.

Glucose Determinations

Prior to each group of assays the membrane covering the tip of the oxygen sensor was removed and replaced with a new membrane. The electrolyte solution was also drained and refilled with fresh electrolyte.

The amperometry cell was assembled and electrical connections made as described in the apparatus section. 10 mL of water were added to the amperometry cell and the stirring rate adjusted to permit efficient stirring. After the stirring rate had been set, tape was placed across the control knob to prevent accidental changes of the setting. To assure a stable stirring rate, the stirring motor was allowed a one hour warm up time. After one hour the water was

drawn out of the cell with a vacuum aspirator and 10.0 mL of glucose solution were placed into the cell with a glass volumetric pipet. The stirring motor was momentarily turned off and after it had slowed sufficiently to engage the stirring bar it was immediately turned on again.

The output of the amplifier was monitored with a digital voltmeter and the output for the first solution was adjusted to 10 V with the trimming resistor. The voltage was observed until it remained stable for one minute at which time the trimming resistor was adjusted slightly to make the output voltage 10 V. The stable voltage output was recorded and the trimming resistor was not adjusted for the remainder of the assays. 10 V represented the voltage output for a solution which contained oxygen at equilibrium with the surrounding air.

The run time was set for 2 min., data acquisition rate 500 ms and the lag time for 10 s. At four seconds prior to the initiation of data acquisition 100 µL of a glucose oxidase solution were pipetted into the cell.

At the end of 2 min the contents of the cell were drawn off with an aspirator and the cell was rinsed 4 times with distilled water and dried with a stream of air. The data corresponding to current output as a function of time were integrated and transferred to disk storage. A hardcopy printout of the difference integral and the time of the minimum completed the run. For a second run 10.0 mL

of a fresh glucose solution were pipeted into the cell and the output voltage of the amplifier was monitored until it leveled off at the voltage corresponding to oxygen equilibration. A new name for the data file was entered and the RETURN key was depressed to start the ten second lag time countdown.

Operating characteristics of the O_2 sensor were studied by adding known amounts of deaerated water to water equilibrated with air and measuring the sensor response. The deaerated water was prepared by bubbling N_2 continuously through 1 L of water at room temperature. The residual current of the sensor was measured by placing the sensor in an oxygen free solution; prepared by adding sufficient Na_2SO_3 to oxidize all dissolved O_2. From these data a detection limit for the electrode was established and the response time of the electrode was determined as a function of pO_2.

Creatine Phophokinase Assays

The ADC was connected as described in the apparatus section. A voltmeter was connected to the input of the ADC and the trimming resistor on the amplifier adjusted to make the amplifier output swing from -10 V to +10 V for left and right full scale deflections of the recording pen on the spectrometer. The reference cell was filled with 3 mL of the CPK auxiliary reaction solution.

It was necessary to determine the quantity of CPK needed to produce response curves ranging from just above the detection limit to a maximum response. In order to do this a sample run was made by adding 100 µL of the stock CPK solution to 2.5 mL CPK auxiliary reaction solution and the absorbance *vs.* time was plotted by the strip chart recorder. The approximate time of inflection was obtained and the time for the absorbance signal to reach a plateau was noted along with the absorbance at the plateau. This information was used to determine if additional CPK needed to be added, if the instrument settings needed to be adjusted, and the expected run time. 100 µL of the least concentrated CPK solution was added to 2.5 mL substrate to see if the response was slightly above the detection limit.

After the proper volume of CPK had been selected the data acquisition program was started. The following quantities were input in response to computer prompting: data acquisition rate, 1 s; run time, 7 min; lag time, 25 s, and a data file name for the current run. Next 2.5 mL of the CPK auxiliary reaction solution were added to a 5 mL beaker with an autopipet. The RETURN key on the Apple was depressed which started the counting cycle. The monitor displayed the time of the countdown by starting with 25 s and counting down by 1 s. An autopipet pipet was used to draw 100 µL of CPK solution. The tip of the pipet was gently wiped with a Kimwipe and at 15 s the aliquot added to the 5 mL beaker. The

Eppendorf pipet was quickly rinsed with the contents of the beaker and the solution mixed by gently swirling for a few seconds. The contents of the 5 mL beaker were then added to the sample cell of the spectrometer and the lid over the cell compartment closed. At this time the countdown was about 4 s, and at zero seconds data acquisition was automatically initiated by the computer.

At the end of seven minutes data acquisition stopped and the data were stored on disk and plotted as a function of time on the monitor screen. The contents of the sample cell were removed by suction and the cell rinsed four times with distilled water. The tip of the suction hose was passed over all the interior walls of the cell to remove any remaining droplets. The 5 mL beaker was rinsed 4 times with water and dried with a Kimwipe. Depressing the RETURN key prepared the computer for another run. After inputting the name of the next file to be save on disk, the RETURN key was depressed again and the countdown routine was started. 100 µL of a CPK solution having a different activity were added 15 s prior to data acquisition. Three consecutive assays at the same CPK activity were performed to check reproducibility.

III. RESULTS

Automatic Pipet Reproducibility Studies

The results of these studies were needed to assist in the choice of the best pipeting device. The RSD for the pipets studied are summarized as follows: 10 mL volumetric glass pipet, 0.06%; variable autopipet adjusted to 5 mL and filled twice to deliver 10 mL, 1%; adjustable autopipet set for 3 mL and filled once, 0.4%.

Response Curves Which Show Maxima

Fluorescence response curves modeling LDH assays were generated using theoretical rate equations. The curves were integrated to demonstrate the efficacy of difference integral calculations to ideal response curves exhibiting maxima. The calculated response simulated the oxidation of lactate in the presence of LDH according to the reaction; lactate + NAD pyruvate + NADH. This is an example of a dehydrogenase single displacement reaction in which lactate and NAD both combine with LDH before any product is formed. The kinetics of this multistep reaction have been studied and a rate equation derived (equation 1) (50).

Figure 8 illustrates fluorescence signal vs. time curves computed from equations 1 and 2 at different LDH concentrations and fixed initial concentrations of lactate and NAD.

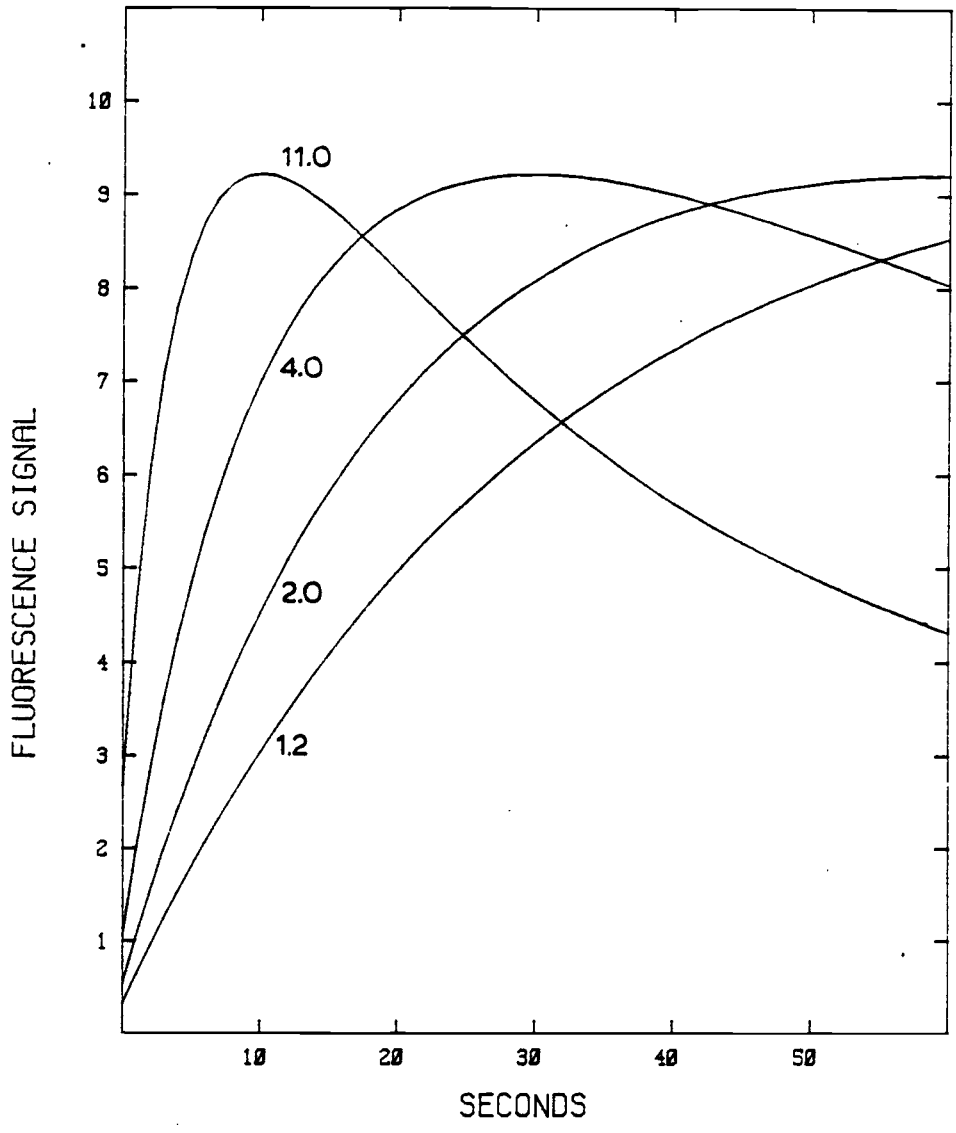

Figure 8

Computer generated fluorescence signal due to NADH as a function of time. These plots were generated using theoretical rate equations for the oxidation of lactate in the presence of LDH. Curves shown are for LDH concentrations of 1.2, 2.0, 4.0, and 11.0 x 10^{-8} M and fixed initial concentrations of 0.1 M NAD and lactate.

Maxima are observed at NADH concentrations greater than 2×10^{-4} M (88) due to pre- and post-filter effects. For curves resulting from LDH concentrations less than 4.2×10^{-8} M, a maximum is not exhibited within the 60 s integration period since the total formation of NADH during this period is less than 2×10^{-4} M. Three characteristics are demonstrated by the curves which have maxima: (1) at higher concentrations of LDH the time of the maximum shifts to smaller values, (2) the magnitude of all maxima are the same, and (3) the rate dependent positive and negative slopes increase in magnitude with increasing LDH concentration. These combined factors indicate the values for the fixed-time difference integrals of response curves with maxima decrease at increased LDH concentration. This is illustrated in Figure 9 where difference integrals are plotted as a function of LDH concentration. At low concentrations of LDH, i.e., less than 4.2×10^{-8} M, the response curves do not traverse a maximum within the 60 s integration period and the magnitude of the integrals increase with increasing LDH concentration. At concentrations of LDH greater than 4.2×10^{-8} M, however, the magnitude of the difference integrals are observed to decrease with increased LDH concentration. Thus difference integral data by themselves are insufficient for determining LDH concentration since a given integral may correspond to two different LDH concentrations.

The time of the maximum is also related to the LDH concentration as shown in Figure 9. An LDH concentration of 4.2×10^{-8} M

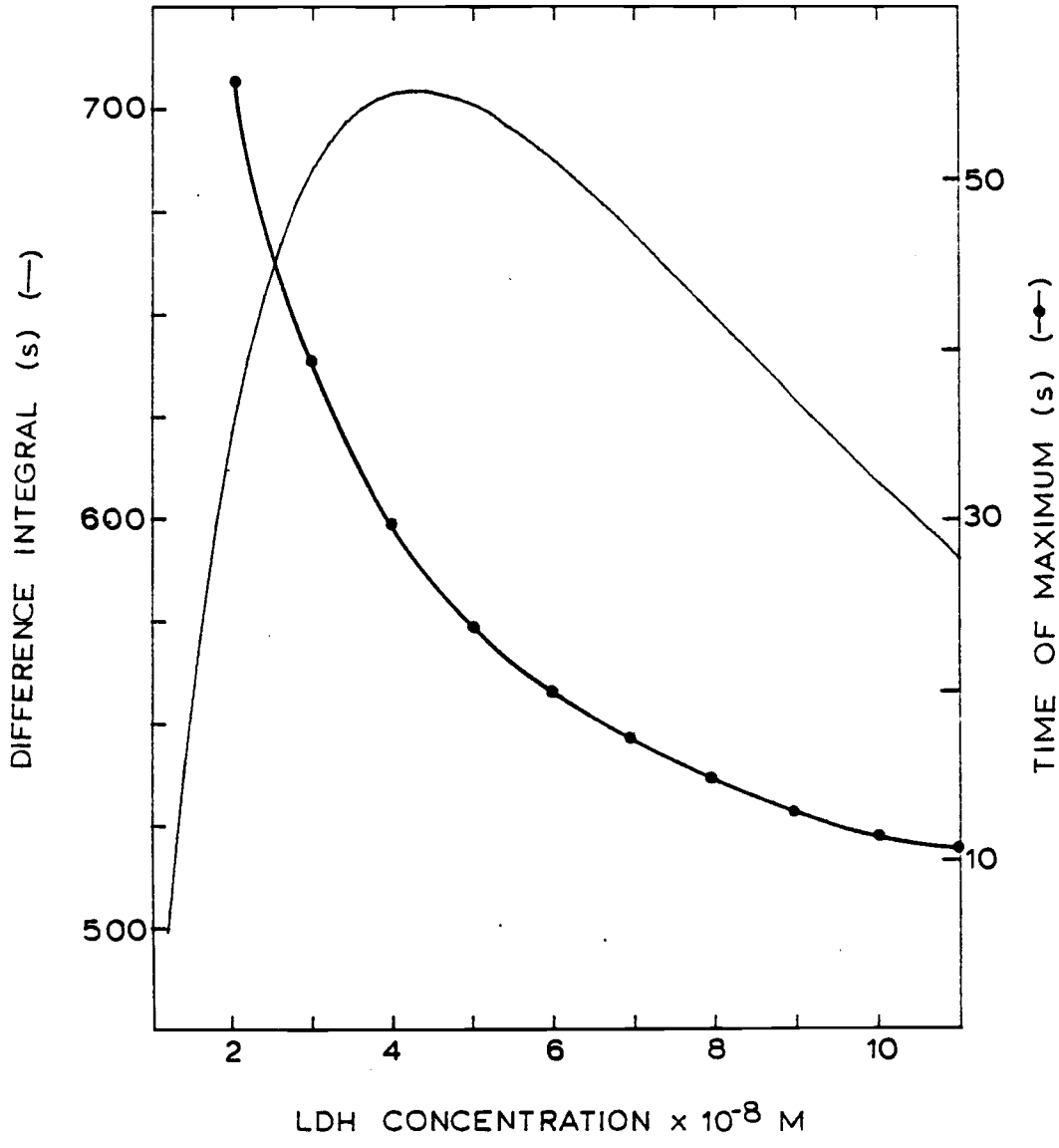

Figure 9
Calculated difference integrals and time of maximum of computer generated plots of NADH for 50 different LDH concentrations. 60 s integration period.

results in a response curve which traverses a maximum at 29 s. Since this is the concentration which yields a maximum integral, those concentrations of LDH which have response curves exhibiting maxima at times less than 29 s correspond to greater concentrations of LDH and have integrals which lie on the right half of the integral curve. Likewise, response curves which do not exhibit a maximum or do exhibit a maximum at times greater than 29 s correspond to lower concentrations of LDH and will have integrals which lie on the left half of the integral curve. Thus, by supplementing the integral data with the time of maximum, it is possible to correlate each difference integral with a unique LDH concentration.

Ethanol Determinations

Ethanol determinations were performed using alcohol dehydrogenase (ADH) to demonstrate the application of difference integral calculations to response curves which exhibit maxima. Ethanol is oxidized in the presence of ADH according to the following equation, ethanol + NAD $\longleftrightarrow$ NADH + acetaldehyde. For these determinations the rate of oxidation was related to the time dependent concentration of ethanol. The reaction kinetics are similar to the LDH reaction used in the theoretical study and discussed above. Reaction progress was monitored by measuring the fluorescence signal due to the rate dependent concentration of the indicator species, NADH.

Ethanol solutions were prepared to include concentrations in the range 50 mg/100 mL to 500 mg ethanol/100 mL, corresponding to blood alcohol levels of interest to forensic chemists and to toxicologists (89). The detection limit was 0.035 mg ethanol/100 mL (7.6 μM).

Initial studies included a scan of excitation and emission wavelengths. The excitation wavelength maximum was found to be 340 nm and the emission wavelength maximum was 474 nm.

Stirring Methods

Methods for stirring were also investigated. Initially a stirring mechanism was built which bubbled N_2 through the cell for a few seconds prior to starting data acquisition. The apparatus was constructed from a 2.5 cm length of glass tubing. One end of the tubing was heated a drawn to capillary dimensions and a 90 degree bend was made in the other end of the tubing. The capillary tube was inserted into the cell out of the optical path and the other end of the tubing was connected to a rubber hose which was connected to a regulated supply of N_2. After the substrate and ADH had been added to the cell, the N_2 was turned on for 4 to drive bubbles through the solution thus mixing it. The N_2 was then turned off prior to data acquisition. Although the method provided adequate stirring, it was difficult to control the rate of bubbling. This resulted in

solution being splattered out of the cell and onto the cell walls. Consequently the bubble stirrer was replaced with the modified stirring motor described in the experimental section.

Figure 10 shows the fluorescence signal vs. time response at three different concentrations of ethanol. Since ADH was added to the substrate 4 s prior to data acquisition the initial 4 s of the reaction was not recorded. This was necessary in order to permit sufficient time to add the ADH and close the cell compartment of the fluorometer. The shapes of these response curves are similiar to those generated from theoretical rate equations shown in Figure 8. The observations cited earlier for the theoretical response curves apply to the curves shown in Figure 10.

A log-log calibration plot over 4 orders of magnitude of concentration is shown in Figure 11. The curve exhibits a maximum at 60 mg/100 mL. Integrals greater than 1475 emission intensity-s may lie of either side of the maximum and therefore must be supplemented with the time of the maximum for proper assignment of concentration. Noting the time of the maximum to be 56 s for the response curve at 60 mg/100 mL, integrals of response curves with times less than 56 s are due to ethanol concentrations greater than 60 mg/100 mL and lie on the right half of the calibration plot. Integrals of response curves not exhibiting a maximum or which do so at times less than 56 s lie on the left half of the curve.

The results of the reproducibility study showed a RSD in the integral of 0.5%. This error results in approximately a 0.6%

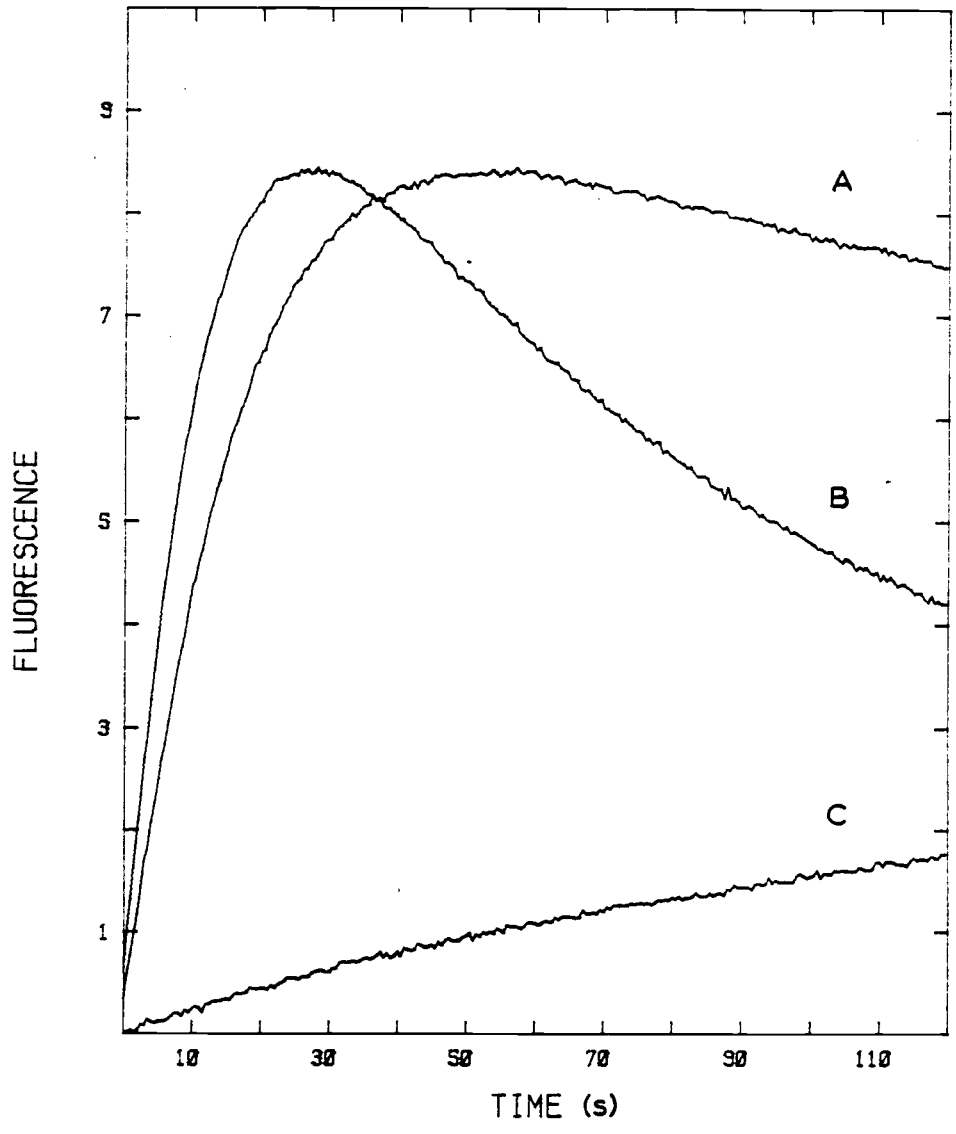

Figure 10
Experimentally measured fluorescence response due to NADH as a function of time for ethanol assays. Initial ADH activities are fixed and ethanol concentrations are (A) 60 mg/100 mL, (B) 600 mg/100 mL, and (C) 1 mg/100 mL.

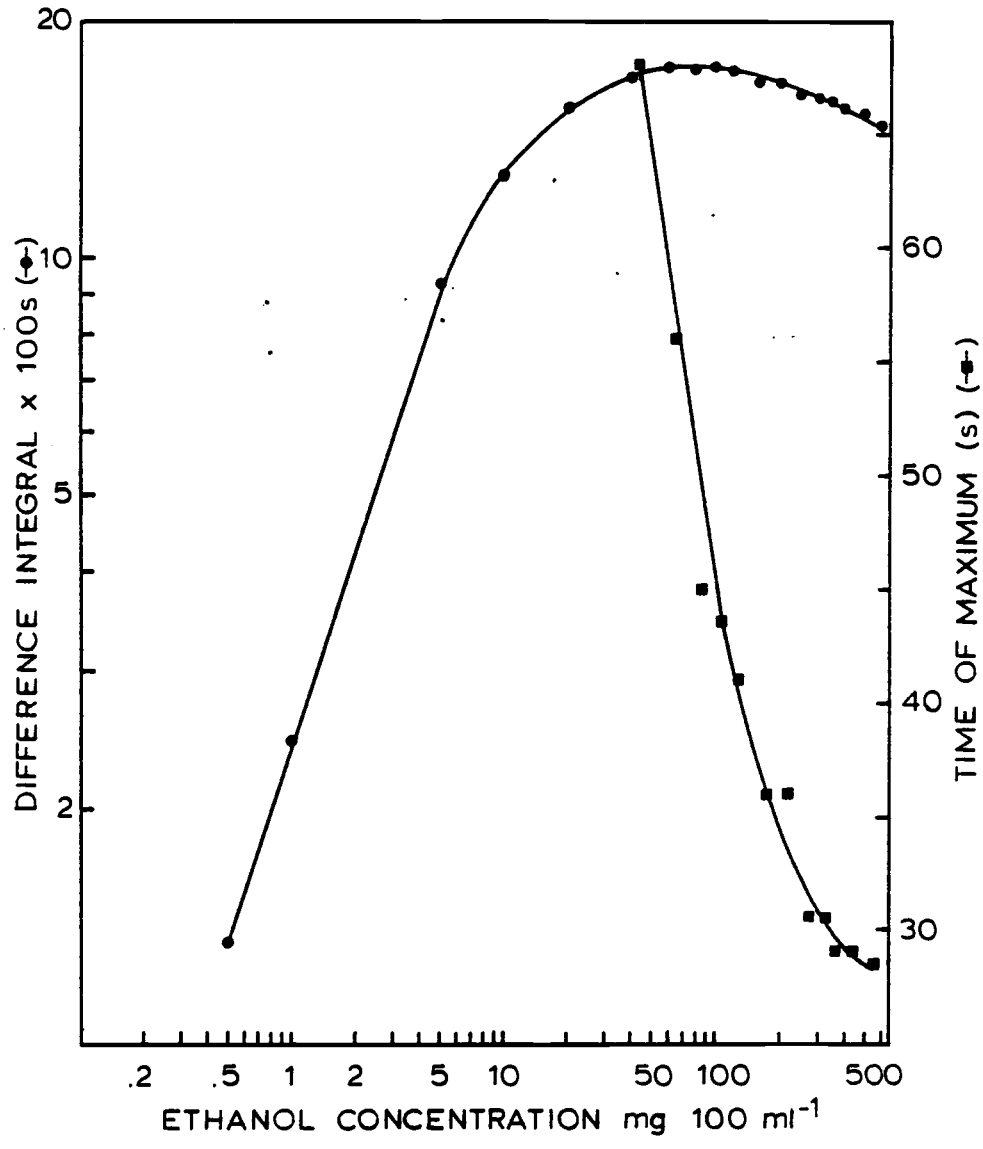

Figure 11
Experimentally determined difference integrals and time of maximum for ethanol concentrations in the range 0.5-600 mg/100 mL. 2 min integration period.

uncertainty in unknown ethanol concentrations below 40 mg/100 mL. At the lower concentrations of ethanol the slope of the integral vs. ethanol curve is steep, thus reducing the error caused from uncertainty in the value of the difference integral. At concentrations which lie on the right half of the integral vs. time curve, however, the slope is very shallow and a 0.5% uncertainty in the integral results in a 5.5% uncertainty in concentration.

Response Curves Which Show Minima

A family of O_2 vs. time curves exhibiting minima were generated using theoretical rate equations. Each curve simulated the time dependent concentration of indicator species, O_2, to be expected during the oxidation of glucose in the prescence of glucose oxidase according to the reaction, glucose + O_2 + H_2O $\longleftrightarrow$ gluconic acid + H_2O_2.

Figure 12 shows theoretical O_2 vs. time curves computed from equations 3-5 at different glucose concentrations and fixed glucose oxidase concentration. A minimum occurs at the point where the rate of diffusion of O_2 into the system from the surrounding environment equals the enzymatic rate of depletion of O_2. For these calculations the decrease in the rate of enzymatic depletion is due to a reduction in the glucose concentration with time.

At increased concentrations of glucose the minimum point of the response curve begins to broaden and form a plateau at an O_2

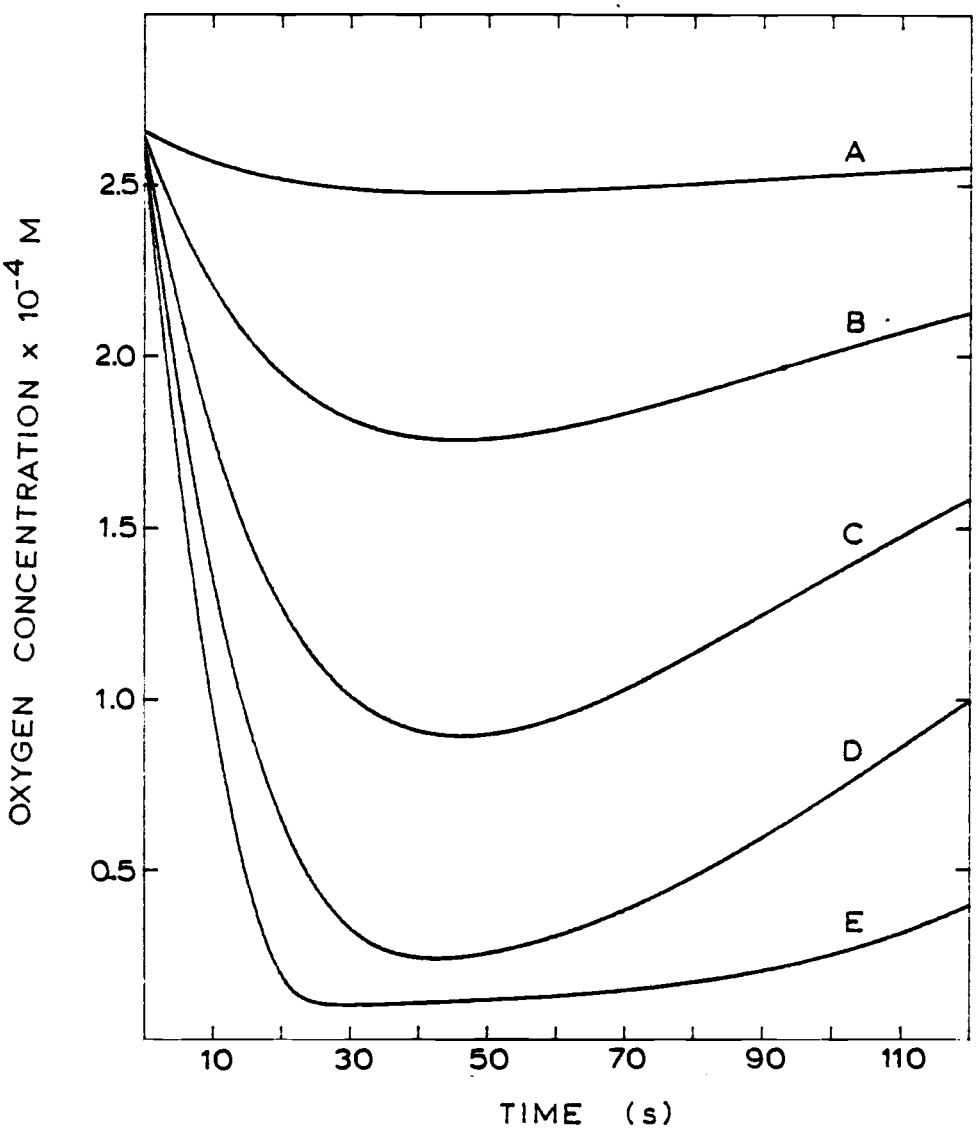

Figure 12

Computer generated $[O_2]$ as a function of time. These curves were generated using theoretical rate equations for the oxidation of glucose in the presence of glucose oxidase. Initial activity of glucose oxidase was fixed and curves shown were for glucose concentrations of; (A) 10^{-4} M, (B) 5×10^{-4} M, (C) 10^{-3} M, (D) 2×10^{-3} M, and (E) 3×10^{-3} M.

concentration of about 2×10^{-5} M. During this time of the reaction there is still sufficient glucose to cause a significant reaction, thus O_2 that diffuses into the solution is quickly used to oxidize the glucose, resulting in a nearly steady-state concentration of O_2. Initially the plateau exhibits a gradually increasing slope due to the diminishing concentration of glucose and concomitant decrease in the enzymatic rate of reaction. When the glucose is entirely depleted the curve begins to rise more steeply since the enzymatic depletion of O_2 is essentially zero and the change in concentration in the solution is governed entirely by the diffusion of O_2 into the solution. At increasing concentrations of glucose, the plateau region remains flat for longer time periods due to excess glucose in solution.

Figure 13 shows difference integrals for 30 theoretical response curves as a function of glucose concentration. The region of linearity extends beyond one order of magnitude followed by significant curvature at concentrations greater than 1.5×10^{-3} M. The region of curvature corresponds to integrals of response curves exhibiting plateau minima. Integrals in this region are very similar since the $[O_2]$ *vs.* time curves are very similar, i.e., a steep negative slope during the first few seconds of the reaction followed by a plateau minimum at the same O_2 concentration. Consequently, integral data are insufficient for determining glucose concentration

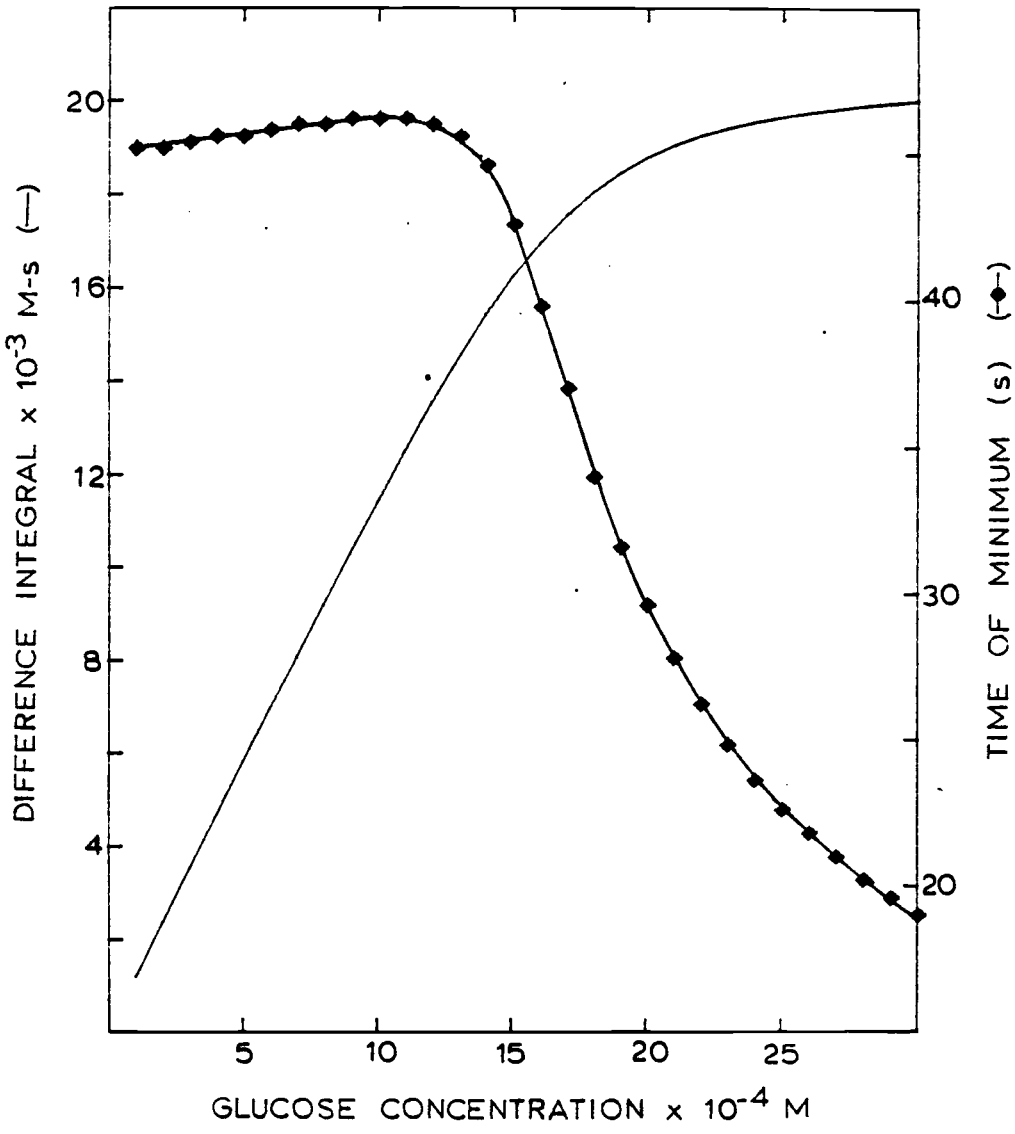

Figure 13
Difference integrals and time of minimum for computer generated $[O_2]$ vs. time function.

at increased concentrations of glucose and supplementary information is necessary to resolve glucose concentrations within this region.

At high concentrations of glucose the time at which the minimum occurs, i.e., the time required to reach the plateau, decreases with increasing concentration of glucose. In addition, the length of the plateau increases with increasing concentration. Therefore the time at which the plateau starts and ends can be used to characterize a given glucose concentration. Since the plateau can be very long (several minutes) at high concentrations of glucose, the time of the minimum was used to resolve glucose concentrations.

Figure 13 also shows the time of the minimum as a function of glucose concentration. At concentrations below 10^{-3} M a minimum in the response curve is traversed at about the same time for each curve, thus making these data less significant for the lower concentrations. This range of glucose concentration, however, can easily be determined from the integral data. As noted previously, glucose concentrations greater than 1.5×10^{-3} M are not easily determined by integral data due to extreme curvature of the calibration plot at increased concentrations of glucose. At these high concentrations of glucose, however, the time of the minimum *vs.* concentration function is only slightly curved and provides a more sensitive measure of glucose concentration. For example, the integral data increases 16% from 1.5×10^{-3} - 2×10^{-3} M, 4% from 2×10^{-3} - 2.5×10^{-3} M and 1.7% from 2.5×10^{-3} - 3×10^{-3} M. Over the same

concentration ranges, however, the time of the minimum increases 30%, 24% and 16%. Therefore the sensitivity of the supplemental derivative function is greater than the sensitivity of the integral function at concentrations greater than 1.5×10^{-3} M. At concentrations of glucose much greater than 3×10^{-3} M the shape of the response curves are essentially independent of glucose concentration.

Glucose Determinations

Glucose oxidase is highly specific for β-D-glucose (1). In order to allow reproducible concentrations of oxidizable glucose, therefore, the solutions were allowed to stand overnight to achieve an equilibrium mixture of 36% alpha and 64% beta (1) by mutarotation.

The initial data for the glucose assays were irreproducible and experiments were conducted to identify the source of the problem. Prior to building the amperometry cell the oxygen sensor was introduced from the top of the beaker. In this position the sensor was perpendicular to solution flow and turbulence caused by the sensor interrupting that flow resulted in bubble formation. The uneven flow around the sensor, resulting in unpredictable mass transfer of O_2, and the presence of bubbles containing O_2 were factors which contributed to the unpredictable response. To alleviate the problem a cell was constructed in which the sensor would not interrupt the

solution flow. The basic design of the cell, described above, introduced the sensor through the wall of the beaker, thus allowing the sensor tip to be flush with the interior wall, preventing it from disturbing solution flow.

Another problem was reproducing the stirring rate. Since the stirring motor had to be slowed to couple to the stirring bar prior to each assay, a mark was placed on the body of the stirring motor permitting readjustment of the rate to the original value after the stirring bar was turning. However, even with careful adjustment of the potentiometer minute changes in the rate resulted. The small changes affected the rate of mass transfer of O_2 to the sensor surface and hence the output of the sensor. This problem was reduced by applying tape to the potentiometer on the stirring motor so that the setting could not accidently be changed and by momentarily disconnecting the power to the stirring motor to allow it to slow and couple to the stirring bar. In addition, the stirring motor was allowed sufficient time to warm up so that temperature fluctuations in the stirring rate were minimized.

In Figure 14 the effect of stirring rate on sensor output, expressed in millivolts, is shown. At rotation rate settings less than 3 and greater than 6 the stirring bar would not couple with the motor. This curve shows that at higher rotation rates, the sensor output is less sensitive to changes in motor speed.

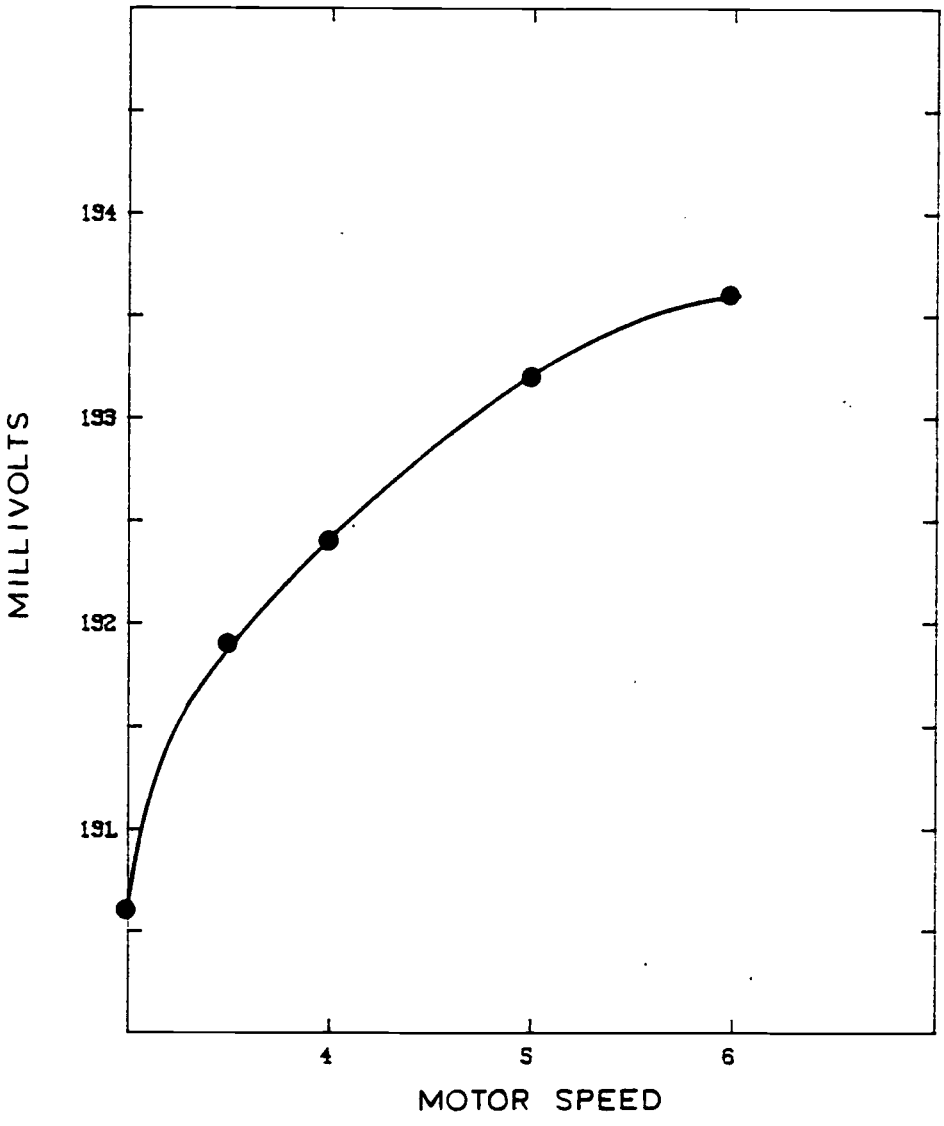

Figure 14
Oxygen sensor output as a function of stirring motor rotation rate. Numbers on abscissa are potentiometer settings.

The ideal working potential of the oxygen sensor was determined by measuring the sensor output as a function of applied potential. From the current vs. potential curve shown in Figure 15 the working potential was chosen at -0.55 V, the approximate midpoint of the O_2 reduction plateau.

The lowest detectable concentration of O_2 should be limited by either the residual current of the sensor or the noise in the sensor output while placed in an oxygen free environment. The residual current output of the sensor was measured in an aqueous solution of Na_2SO_3. Sulfite quickly reduces O_2 and excess Na_2SO_3 was added to ensure the reduction of O_2 which diffuses into the solution from the surrounding environment during the measurement time. The residual current was significantly lower (88%) than the current output in a 90% deaereated solution. Therefore, the detection limit was determined from the noise in the output current. The detection limit was 1.1 ppb (3.5×10^{-8} M O_2) and was calculated from the standard deviation of the sensor current output in the Na_2SO_3 solution and a calibration plot of % deaereated water vs. sensor output.

The response time for the sensor is a function of the change in O_2 concentration as shown in Figure 16. For these data, the time required for the sensor to change from equilibrium output to 90% of the final output for a solution of deaereated water was measured for

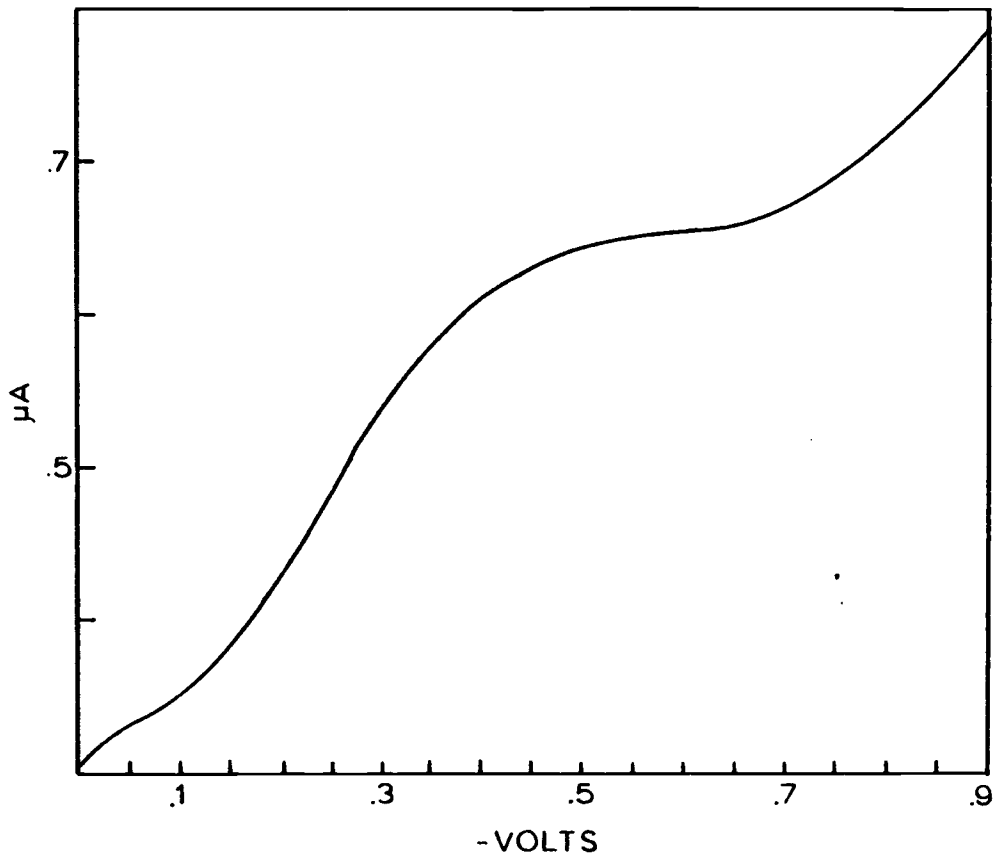

Figure 15
Sensor output current as a function of working potential.

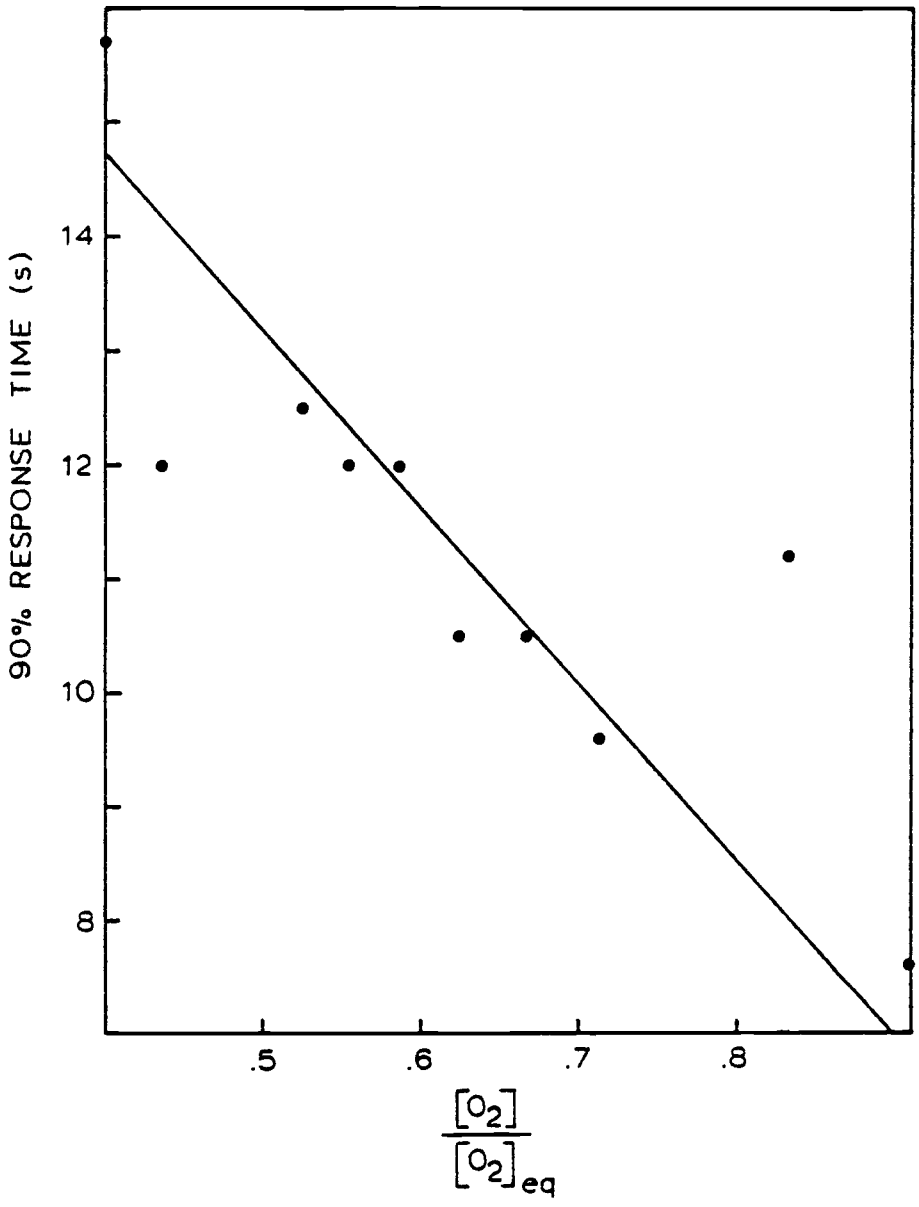

Figure 16
Time for sensor output to achieve a 90% maximum response as a function of changes in O_2 concentration.

several aqueous solutions of % O_2. As the change in O_2 concentration increases, the response time of the electrode increases.

Figure 17 shows O_2 current *vs.* time curves at several different glucose concentrations and a fixed glucose oxidase activity. Although the initial current value is different for some of the latter curves, the difference integral is not affected by a change in the initial values. Plots of the difference integrals as a function of glucose concentration are shown in Figure 18. At concentrations of glucose less than 1 mM difference integrals are nearly linear with glucose concentration and correspond to O_2 current curves which traverse a distinct minimum. At concentrations greater than 10^{-3} M, however, the O_2 current curves (see Figure 17) merge along a plateau minimum, resulting in similar values for the difference integrals. In Figure 18, therefore, the curve shows noticeable curvature at these glucose concentrations. The time of the minima are plotted as a function of glucose concentration in Figure 18 and reveal a slightly more sensitive measure of glucose concentration for concentrations greater than 10^{-3} M.

Response Curves Which Show Inflection Points

Families of theoretical [NADPH] *vs.* time curves exhibiting inflection points were generated using published rate equations (50, 52, 53). The curves modeled CPK assays by simulating the time

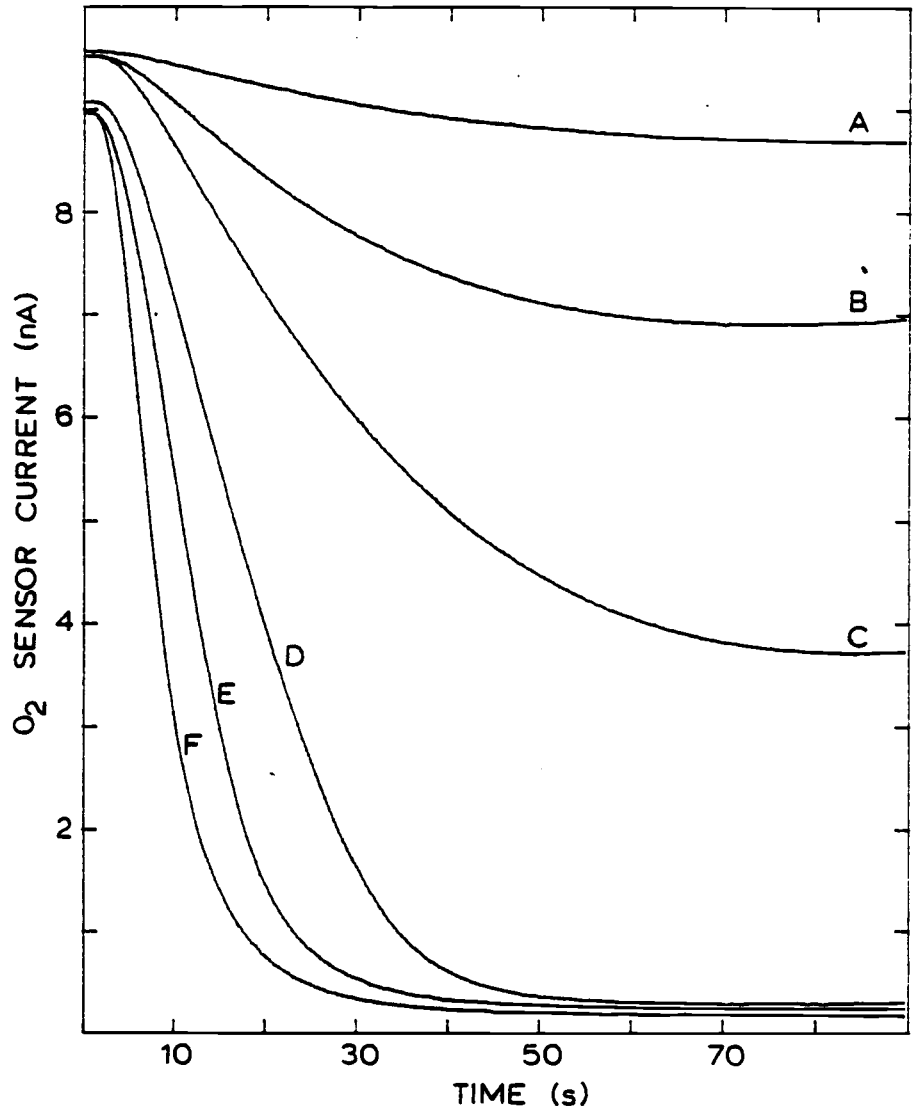

Figure 17
Results of glucose determinations. Sensor response as a function of time for fixed glucose oxidase activity and glucose concentrations of (A) 10^{-4} M, (B) 4×10^{-4} M, (C) 8×10^{-4} M, (D) 2×10^{-3} M, (E) 4×10^{3} M, and (F) 10^{-2} M.

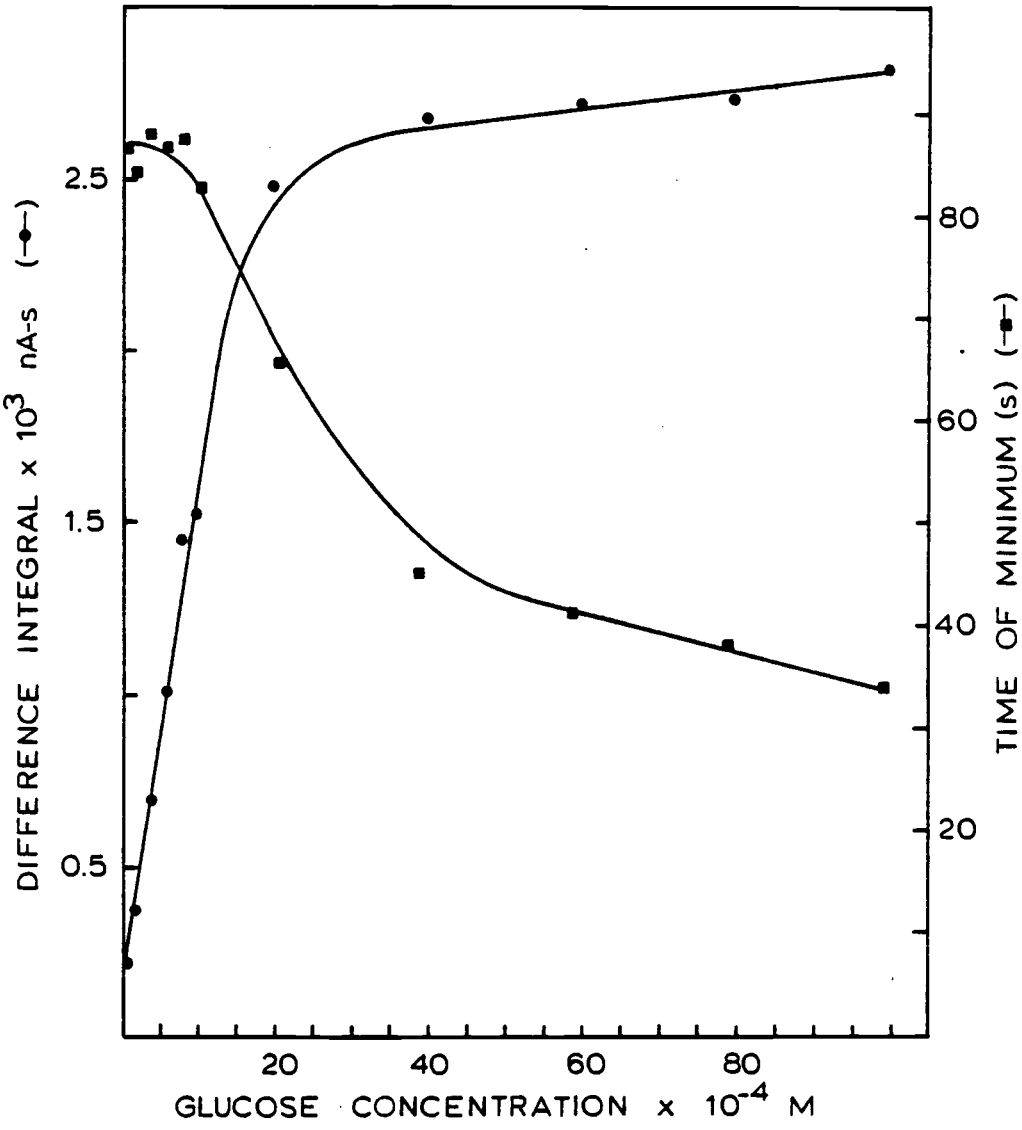

Figure 18
Difference integrals and time of minimum of sensor response for glucose determinations.

dependent concentration of indicator species, NADPH, resulting from a coupled consecutive reaction:

$$\text{ADP} + \text{Creatine Phosphate} \overset{\text{CPK}}{\longleftrightarrow} \text{Creatine} + \text{ATP}$$

$$\text{ATP} + \text{Glucose} \overset{\text{HK}}{\longleftrightarrow} \text{Glucose-6-Phosphate (GPD)} + \text{ADP}$$

$$\text{G6P} + \text{NADP} \overset{\text{GGPD}}{\longleftrightarrow} 6\ \text{Phosphogluconate} + \text{NADPH}$$

The first two reactions are linked by ATP and the final two by G6P. Increasing the concentration of CPK increases substrate concentration in the final two reactions resulting in an increased rate of NADPH formation.

Figure 19 shows [NADPH] vs. time curves generated from kinetic data (50, 52, 53) for varied CPK concentration and all other initial concentrations fixed. The initial concentrations of ATP, G6P and NADPH are zero for the first few seconds of the reaction, resulting in a lag phase or induction period. This is typical of consecutive reactions and occurs when the indicator species is not immediately formed at the initiation of the reaction but after time as allowed the buildup of intermediates (90). The rates of the final two reactions are dependent, among other factors, on the concentration of intermediates ATP and G6P, respectively. During the induction period the intermediate concentrations are low and the reaction proceeds at a negligible rate. Accumulation of G6P, however, increases

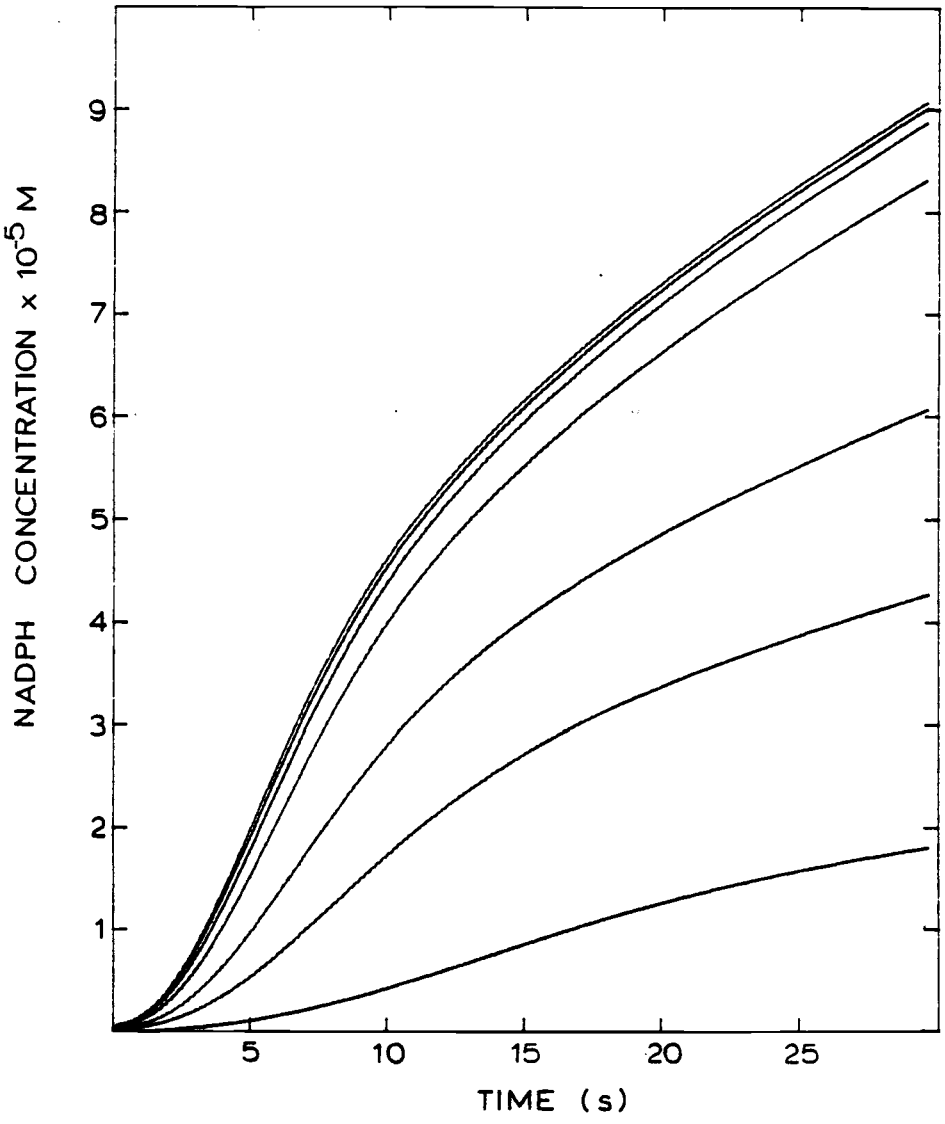

Figure 19

Computer generated NADPH vs. time curves. These curves were generated using theoretical rate equations for the CPK coupled reactions. From the top curve to the bottom, CPK quantities are 0.5, 0.4, 0.3, 0.2, 0.1, 0.05 and 0.01 μg.

the rate at which NADPH is formed, causing a steep rise in the response curve. Substrate depletion causes the response curve to level off, resulting in an inflection point.

At increased concentrations of CPK, ATP and G6P are produced at increased rates, thus decreasing the time of the lag phase and increasing the rate at which NADPH is formed. The inflection point, therefore, is more distinct and occurs at shorter periods of time.

The overall rate at which NADPH is produced is limited by the slowest step in the reaction. At low CPK activities this is the step catalyzed by CPK. At higher CPK activities, however, the rate of this step increases and the reaction is expected to be limited by one of the auxiliary reactions. The rate of NADPH formation therefore becomes increasingly independent of CPK activity and the response curves tend to merge at increased activities of CPK. The rate of NADPH formation would not be expected to be entirely independent of CPK activity, however, since the rate limiting step is partially a function of the concentration of intermediates produced by the reaction catalyzed by CPK.

At low concentrations of CPK the rate at which NADPH is formed is limited by CPK concentration and the reaction is slower and the response curve exhibits a longer lag phase and a more diffuse inflection point.

Figure 20 shows difference integrals as a function of CPK concentration. As expected from the response curves, the integral

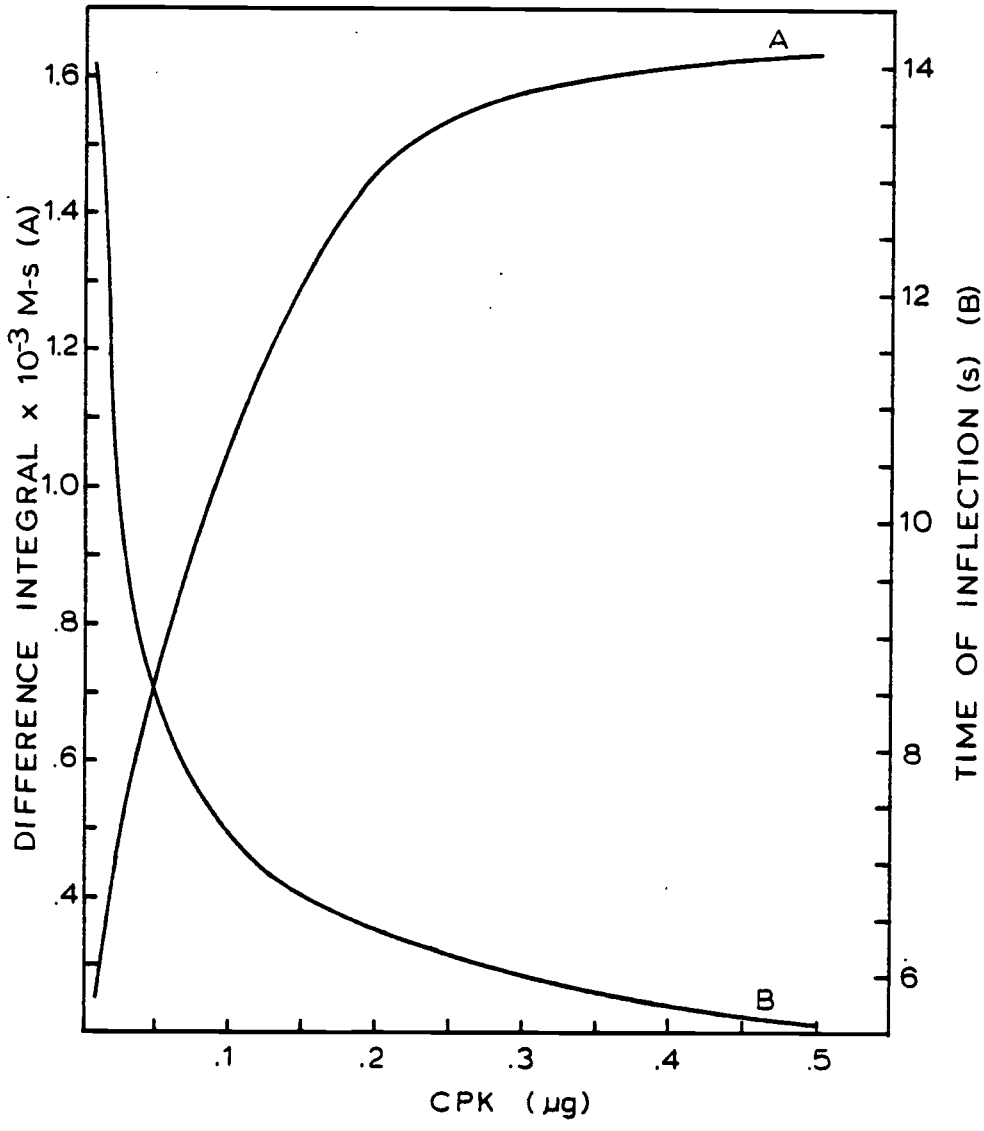

Figure 20
Difference intergrals (A) and time of inflection (B) of computer generated NADPH vs. time curves.

curve levels off at increased concentrations of CPK due to the increasing independence of CPK on the shape of the response curve.

Inspection of the response curves suggests that the time of the inflection point is not helpful in resolving CPK concentrations. Figure 20 also shows the time of inflection as a function of CPK concentration, supporting this suggestion. At increased concentration of CPK the inflection point changes only slightly since the rate of reaction becomes increasingly independent of CPK concentration.

CPK Assays

CPK assays were performed to demonstrate the application of difference integral calculations to a real system exhibitng an inflection point. CPK assays are significant in clinical laboratories and are used as a diagnosis of myocardial infarcation (1). With the concentrations of substrates and enzymes used in this study it was possible to measure CPK activity over three orders of magnitude. The detection limit was 10^{-3} units CPK.

The absorbance of NADPH as a function of time is shown in Figure 21. The initial 15 s of the reaction were not monitored since solutions had to be mixed and placed into the sample cell during this time. The observations for the assays are the same as for the theoretical calculations, i.e., at increased activities of CPK the inflection point becomes more distinct and the response curves become closer together and nearly merge.

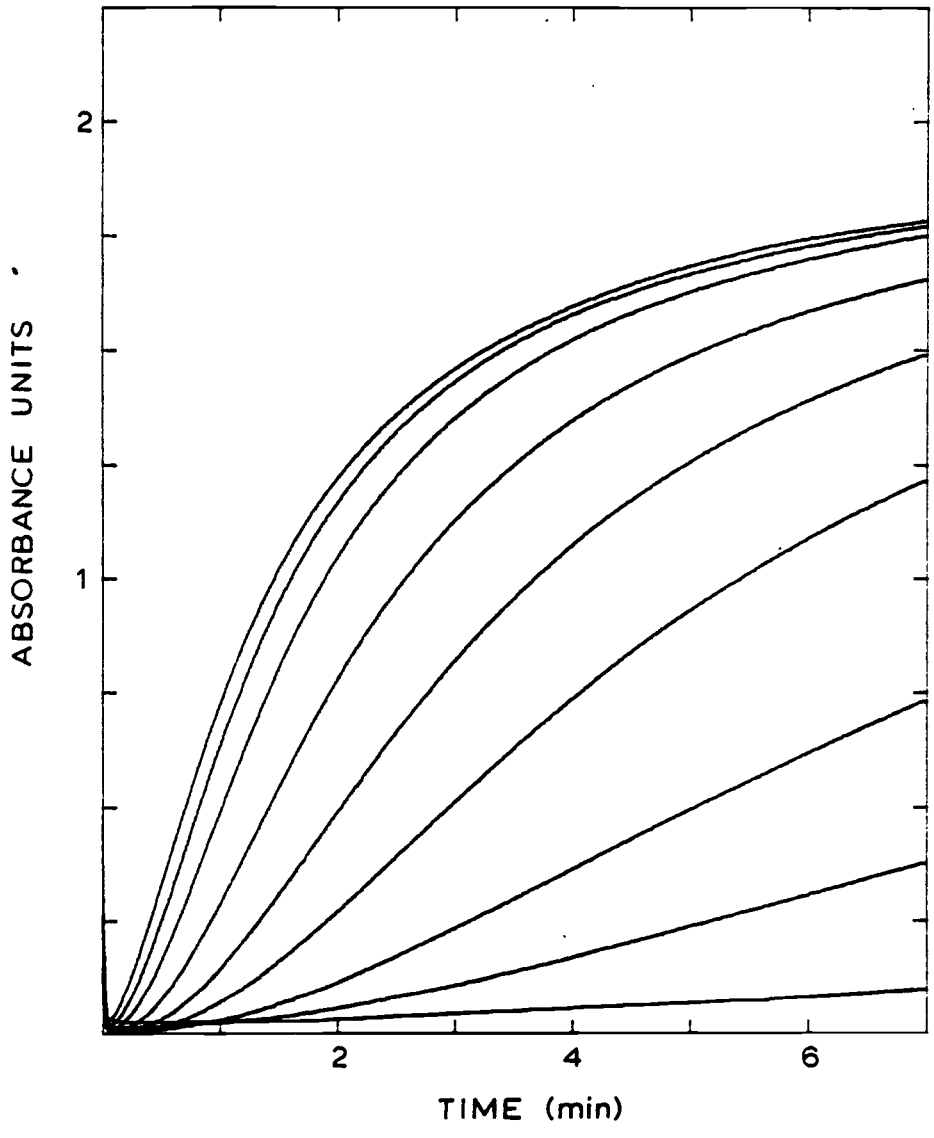

Figure 21
Results of CPK assays. Absorbance due to NADPH as a function of time. From bottom to top CPK activities are 0.1, 0.5, 1, 2.5, 5, 10, 25, 50 and 100 units.

The reproducibility of three identical samples at CPK activity of 10 units shows integrals with a RSD of 2.2%. A significant portion of this error could be attributed to the long analysis time (7 min) and accompanying temperature fluctuations during that time.

Figure 22 shows difference integrals as a function of CPK activity. At concentrations of CPK 0.01 units and below there exists sufficient sensitivity to correlate the integral with CPK activity. At concentrations of CPK greater than 0.1 units, however, the slope of the curve quickly falls off making integral data in this region less useful. At these elevated activities of CPK the response curves tend to merge, thus the integrals asymptotically approach the same value.

As shown in Figure 22, the time of inflection decreases with increasing CPK concentration. The sensitivity of this function, however, is less than the sensitivity of the integral function at high CPK activities. These observations are consistent with the theoretical results discussed above.

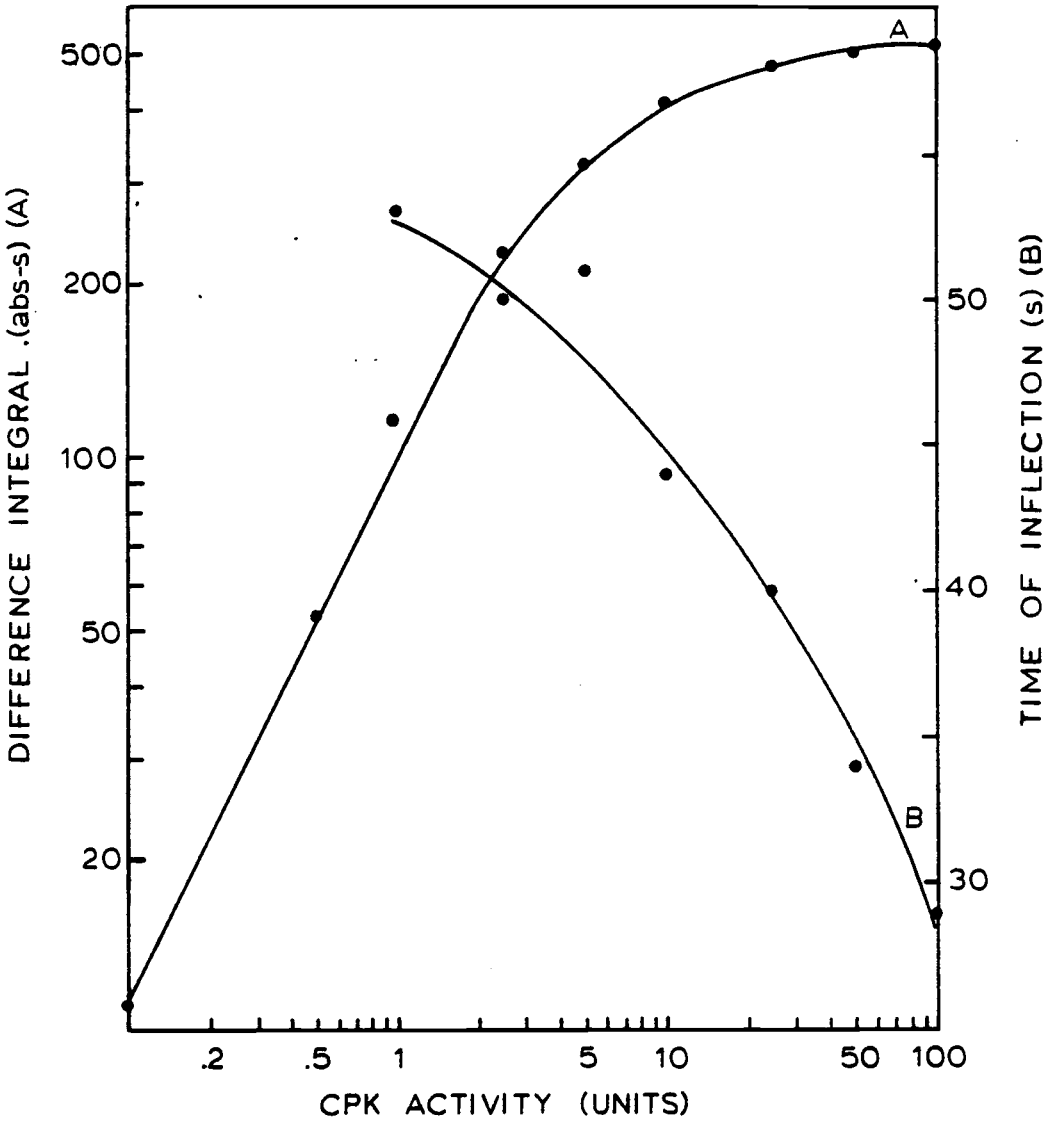

Figure 22
Difference integrals (A) and time of inflection (B) for CPK assays.

IV. CONCLUSIONS

Restrictions upon kinetic methods of analyses frequently accompany their use. For example, most methods can only be applied to that portion of the response curve which is linear, thereby limiting those methods to zero or pseudo first-order kinetics; often at the imposition of costly amounts of excess enzyme or substrate. Multipoint methods may be applied to nonlinear response curves although the fitting of the initial rate data to a mathematical model presumes the kinetics of the reaction are well understood, and thus restricts the number of systems to which this method may be applied.

The interval integration method described by Thomas is a versatile method and general in its applications. Kinetic data may be obtained from the linear and nonlinear portion of the response curve without the requirement of additional kinetic information. This research has extended the utility of this method to include response curves which exhibit maxima, minima or inflection points, thus permitting analyses of virtually all types of kinetic response data.

The choice of analytical instrumentation and particular enzyme systems resulted in response vs. time curves having maxima, minima or inflection points. Response curves were integrated over a fixed-time interval which included the region where the first or second derivative was zero. Difference integrals were calculated and

related to enzyme activity or substrate concentration. The resulting calibration plots of difference integral vs. concentration or activity were double- or single-valued, depending upon the nature of the response data.

For response curves which show a maximum at a constant amplitude, increasing the reaction rate by increased concentration of substate or enzyme results in response curves with decreasing integrals. Therefore, the integral data are double-valued, with integrals along the positive slope corresponding to lower analyte concentrations and integrals along the negative slope corresponding to greater concentrations. Since a one-to-one correlation of difference integrals with analyte concentration is not evident in a double-valued integral plot, additional information is necessary which would permit the correlation. It was noted that response curves which do not exhibit a maximum lie on the left half of the integral curve. Therefore a simple derivative test is sufficient to correlate these curves, i.e., if a response curve does not go through a maximum, the integral will lie on the left half of the calibration plot.

A more general approach is to use the time at which a response curve traverses a maximum. By noting the time for the response curve with the largest integral and comparing the time of the maxima of each response curve, each integral may be correlated to a unique analyte concentration. For example, if the time of the maximum is

less than the time of maximum for the largest integral, then the integral will lie on the right half of the calibration plot; if the time of the maximum is greater, the integral will lie on the left half.

For response curves which do not exhibit a minimum point but a minimum plateau instead, increased analyte concentration lengthens the plateau and results in slightly increased difference integrals and hence a calibration curve which asymtotically approaches a maximum value. Since the sensitivity of the calibration plot decreases at increased analyte concentration, the time at which the minimum occurs in the response curve was used to supplement integral data as a more sensitive measure of analyte concentration over a limited concentration range.

For response curves which exhibit inflection points, difference integrals were single-valued functions of analyte concentration. At increased analyte concentration the response curves merged, resulting in an assymptotical calibration curve.

With this integration method of analysis, detection limits may be a function of time. That is, as analysis time increases, the total concentration of indicator species and hence the value of the difference integral also increases. Since the integral of the standard deviation of the noise also increases with time, improvements in the detection limit may be realized only if the integral of the

response signal increases more rapidly than the integral of the standard deviation of the noise.

Although integration methods frequently result in nonlinear calibration plots, the advantages to be gained from this method include fewer restrictions in the choice of instrumentation, the choice of enzyme systems to be assayed, analysis time periods, and quantities of enzymes and substrates used in assays. In addition, less reliance on manual interpretation of data and increased use of computers has nurtured increased acceptance of nonlinear relationships (43).

Suggestions for Future Research

This research has answered questions regarding the use of integration methods with complicated enzyme systems. Additional research, however, could address other questions regarding integration methods. For example, a comparison could be made between integration methods and the other kinetic methods discussed earlier. This research would be beneficial in assessing the relative merits of each method and would be useful to workers needing to select a kinetic method for a particular assay. The comparison could include a study of the relative reproducibilities, accuracy, ease of analysis, required analysis time, effects of interferences, and inherent restrictions of each method.

Optimization of experimental variables such as pH and temperature and a study of the sensitivity of integration methods to these variables could also be included in future research. In addition, a study could be performed to find optimum integration times for reducing noise through signal averaging.

Since many of the calibration plots resulting from integration methods are nonlinear, research could be directed to find ways to more effectively utilize these data. For example, fitting the data to a mathematical function would provide a reliable means for calculating activity. Integration periods could also be varied, i.e., made longer or shorter to increase the dynamic range of the calibration function.

The application of integration methods to other systems could also be investigated. For example, integration methods may be used for assays for inorganic catalysts. In addition, antibody concentrations may be determined by using integration methods for enzyme multiplied immunoassay techniques (EMIT).

V. REFERENCES

(1) N.W. Tietz ed. in Fundamentals of Clinical Chemistry, W.B. Saunders Co., Philadelphia, (1970).

(2) J. Ladue, F. Wroblewski and A Karmen, Science 120 (1954) 497.

(3) Manual of Clinical Enzyme Measurements, Worthington Biochemicals, Freehold N.J., 1971.

(4) G.C. Guilbault in: Handbook of Enzymatic Analysis, Marcel Decker, New York, 1976.

(5) F. Mizutani, K. Saski and Y, Shimura, Anal. Chem. 55 (1983) 35.

(6) D.G. Hoel, N.L. Kaplan and M.W. Anderson, Science 219 (1983) 1032.

(7) J. Schormuller in: Methods of Enzymatic Analysis, Springer Verlag, Berlin, 1974.

(8) W. Haab and L. Smith J., Dairy Sci. 39 (1959) 1644.

(9) Ibid. 40 (1957) 546.

(10) I. Fatt in: Polarographic Oxygen Sensors, CRC Press, Cleveland, Ohio, 1976.

(11) H.L. Pardue, Clin. Chem. 23 (1977) 2189.

(12) H.A. Mottola and H.B. Mark, Jr., Anal. Chem. 52 (1980) 31R.

(13) H.A. Mottola and H.B. Mark Jr., Anal. Chem 54 (1982) 62R.

(14) A. Polkis and M.A. Mackell, Clin. Chem. 28 (1982) 2125.

(15) P.W. Carr and L.D. Bowers in: Immobilized Enzymes in Analytical and Clinical Chemistry, John Wiley and Sons, New York, (1980), Chapter 3.

(16) A.C. Javier, S.R. Crouch and H.V. Malmstadt, Anal. Chem. 41 (1969) 239.

(17) E.A. Robertson, E. Wright, R.A. Chesler and R.J. Elin, Clin. Chem 28 (1982) 2106.

(18) P.W. Carr, Anal. Chem. 50 (1978) 1603.

(19) J.D. Ingle, Jr. and S.R. Crouch, Anal Chem. 42 (1970) 1055.

(20) J.D. Ingle and S.R. Crouch, Anal. Chem. 43 (1971) 697.

(21) J.D. Ingle and S.R. Crouch, Anal. Chem. 45 (1973) 333.

(22) G.E. James and H.L. Pardue, Anal. Chem. 41 (1969) 1618.

(23) H.L. Pardue and B. Fields, Anal. Chim. Acta 124 (1981) 39.

(24) H.L. Pardue and B. Fields, Anal. Chim. Acta 124 (1981) 65.

(25) C. Dellamonica, C. Collombel, J. Cotte and P. Addis, Clin. Chem. 29 (1983) 161.

(26) J.D.H. Cooper, D.C. Turnell and C.P. Price, Clin. Chim. Acta 126 (1982) 297.

(27) M.W. Sundberg et. al., Clin. Chem. 29 (1983) 645.

(28) S.C. Good and R.J. Mathews, Anal. Chem. 50 (1978) 1608.

(29) R.H. Callicott and P.W. Carr, Anal. Chem. 46 (1974) 1840.

(30) H.V. Malmstadt and S.R. Crouch, J. Chem Ed. 43 (1966) 340.

(31) I.F. Dolmanova et. al., J of Anal. Chem. USSR (Translated) 34 (1979) 1275.

(32) I.I. Alekseeva et al., J. of Anal. Chem. USSR (Translated) 35 (1980) 43.

(33) R.P. Igov, M.D. Jaredia and T.G. Pecev, Talanta 27 (1979) 361.

(34) H. Weisz and G. Fritz, Anal. Chim. Acta 123 (1981) 239.

(35) S. Pantel and H. Weisz, Anal. Chim. Acta 109 (1979) 351.

(36) R.E. Adams and P.W. Carr, Anal. Chem. 50 (1978) 944.

(37) R.E. Adams, S.R. Betso and P.W. Carr, Anal. Chem. 48 (1976) 1989.

(38) L.C. Thomas and G.D. Christian, Anal. Chim. Acta 77 (1975) 153.

(39) E.S. Iracki and H.V. Malmstadt, Anal. Chem. 45 (1973) 1766.

(40) E.M. Cordos, S.R. Crouch, and H.V. Malmstadt, Anal. Chem. 40 (1968) 1812.

(41) S.D. Hamilton and H.L. Pardue, Clin. Chem. 28 (1982) 2359.

(42) J.D. Lin and H.L. Pardue, Clin. Chem. 28 (1982) 2081.

(43) H.L. Pardue, J. Pure and App. Chem 54 (1982) 2035.

(44) R.S. Harner and H.L. Pardue, Anal. Chim. Acta 127 (1981) 23.

(45) G.E. Mieling and H.L. Pardue, Anal. Chem. 50 (1978) 1611.

(46) G.E. Mieling, H.L. Pardue, J.E. Thompson and R.A. Smith, Clin. Chem. 25 (1979) 1581.

(47) K.A. Conners, Anal. Chem. 51 (1979) 1155.

(48) S.A. Schubert, J.W. Clayton and Q. Fernando, Anal. Chem. 52 (1980) 963.

(49) E. Mentasti, Anal. Chim. Acta 111 (1979) 177.

(50) V. Bloomfield, L. Peller, and R.A. Alberty, J. Amer. Chem. Soc. 84 (1962) 4367, 4375.

(51) F.R. Duke, M. Weber, D.S. Page, V.G. Bulgrin and J. Luthy, J. Amer. Chem. Soc. 91 (1969) 3904.

(52) G.G. Hammes and D. Kochavi, J. Amer. Chem. Soc. 84 (1962) 2069.

(53) J.F. Morrison and E. James, Biochem J. 97 (1965) 37.

(54) A.J. Brown, J. Chem. Soc. (Trans) 61 (1982) 369.

(55) A.J. Brown J., Chem Soc. (Trans) 81 (1902) 373.

(56) V. Henri and C.R. Hebd. Seanc. Acad. Sci. (Paris) 135 (1902) 916.

(57) V. Henri in: Lois Generales de L'action des Diastases, Hermann, Paris, 1903.

(58) L. Michaelis and M. Menton, Biochem. Z. 49 (1913) 333.

(59) C. Walter in: Steady State Applications in Enzyme Kinetics, Ronald Press Co., New York, 1965.

(60) A.L. Lehninger in: Biochemistry, Worth Publishers, New York, 1975.

(61) I.H. Segel in: Enzyme Kinetics, John Wiley and Sons, New York, 1975.

(62) K. Dalziel, Acta Shemica Scandanavia 11 (1957) 1706.

(63) C.L. King and C. Altman, J. Amer. Chem. Soc. 60 (1956) 1375.

(64) W.W. Cleland, Biochem. Biophys. Acta 67 (1963) 188.

(65) A.H. Gutfreund, Can. J. of Biochem. 58 (1980) 1.

(66) C. Walsh in: Enzymatic Reaction Mechanisms, W.H. Freeman and Company, San Francisco, 1979.

(67) V. Massey and C.H. Williams, ed's in: Flavins and Flavoproteins, Elsevier, New York, 1982.

(68) J.P. Baumberger, Am. J. of Physiology 129 (1940) 308.

(69) P.W. Davies and F. Brink Jr., Review of Scientific Instruments 13 (1942) 524.

(70) L.C. Clark Jr., Trans. Am. Soc. Artif. Intern. Organs 2 (1956) 41-48.

(71) O.J. Jensen, T. Jacobsen and K. Thompson, J. Electroanalytical Chem. 87 (1978) 203.

(72) A. Berkenbosh, Acta Physiol, Pharmacol. Neerl. 14 (1967) 300.

(73) A.J. Bard and L.F. Faulkner in: Electrochemical Methods, John Wiley and Sons, New York, 1980.

(74) N. Lakshiminarayanaiah in: Membrane Electrodes Academic Press, New York, 1976.

(75) E. Gnaiger and N. Forstner Ed's in: Polarographic Oxygen Sensors Aquatic and Physiological Applications, Springer-Verlag Berglin Heidelberg, New York, 1983.

(76) D.W. Van Kreuelen in: Properties of Polymers, Elsevier, Amsterdam 1972, p. 286.

(77) Beckman Owners Manual for Oxygen Sensors, 1979.

(78) M.L. Hitchman and S. Kauser, Anal. Chim. Acta 143 (1982) 131.

(79) I. Karube et. al., Anal. Chim. Acta 119 (1980) 271.

(80) F. Mizutani et. al., Anal. Chim. Acta 118 (1980) 65.

(81) T. Yao, Anal. Chim. Acta 148 (1983) 27.

(82) F. Mizutani and K. Tsuda, Anal. Chim. Acta 139 (1982) 359.

(83) N.W. Rhodes, Byte Magazine March (1982) 414.

(84) A. Schwartz in: Calculus and Analytic Geometry, Holt, Rinehart, and Winston, New York, 1967.

(85) J.D. Ingle Jr., Chemistry 520 Class notes, Oregon State University, 1982.

(86) L.C. Thomas and G.D. Christian, Anal. Chim. Acta 89 (1977) 83.

(87) A. Savitzky and M. Golay, Anal. Chem. 36 (1964) 1627.

(88) H.K. Willard, L.L. Merrit Jr., J.A. Dean and F.R. Settle Jr. in: Instrumental methods of Analysis, Wadsworth Publishing, Belmont, CA., 1981, p. 110.

(89) J. Doull, C.D. Klaassen and M.O. Amdur Ed's, in Casarett and Doull's Toxicology, MacMillan Publishers, New York, 1980.

(90) J.H. Espenson in: Chemical Kinetics and Reaction Mechanisms, McGraw Hill, 1981, p. 66.

APPENDICES

APPENDIX 1
LIST OF SYMBOLS

abs	absorbance units
ACR	auxiliary control register
ADH	alcohol dehydrogenase
ADP	adenosine diphosphate
AMP	adenosine monophosphate
ATP	adenonsine triphosphate
CLI	clear interrupts
CPR	creatine phosphokinase
DIM	dimension
DME	dropping mercury electrode
DOS	disk operating system
G.O.	glucose oxidase
G6PD	glucose-6-phosphate dehydrogenase
G6P	glucose-6-phospate
HK	hexokinase
IER	interrupt enable register
IFR	interrupt flag register
I/O	input/output
IRQ	interrupt request
K_M	Michaelis-Menten constant
M	molar concentration

mM	millimolar
ms	milliseconds
NAD	nicotinamide-adenine dinucleotide
DADP	nicotinamide-adenine dinucleotide phosphate
NADPH	reduced nicotinamide-adenine dinucleotide phosphate
NMI	nonmaskable interrupt
ns	nanoseconds
pO_2	oxygen tension
PCR	peripheral control register
PROM	programmable read only memory
RAM	random access memory
ROM	read only memory
s	seconds
V_{max}	maximum reaction rate
$	hexadecimal
ul	microliters

APPENDIX 2
Data Acquisition Program

```
5  REM  SET ASIDE MEMORY FOR BASIC AND DATA STORAGE
10  LOMEM: 24576: HIMEM: 38233
15  REM  LOAD MACHINE LANGUAGE PROGRAM AND INTERRUPT VECTORS
20  PRINT  CHR$ (4);"BLOADTIMES"
30  POKE 1019,76: POKE 1020,134: POKE 1021,149
40  INPUT "TIME  ";R1
50 Z1 = 19.1:Z2 = 191
60 D$ =  CHR$ (4)
70  INPUT "LAG TIME IN SECONDS  ";R
80  INPUT "SAMPLING RATE IN MS  ";B
90  INPUT "RUN TIME IN MINUTES  ";C
100  INPUT "NUMBER OF POINTS PER LEAST SQUARES ANALYSIS  ";J4
110  INPUT "MAX (1), MIN (2)  ";M8
120  GOSUB 1080
130 D = B / 1000:P = .00015:N = C * 60000 / B
140 J2 = 1:J3 = J4:L = N - J4: DIM Z$(30)
150 N1 = N: DIM Y(N):B = B / 10
160 B1 = B: DIM IN(30): DIM SL(L)
170  GOTO 190
175  REM  ENABLE INTERRUPTS
180  CALL 38268: RETURN
190  INPUT "DO YOU WISH TO TAKE BLANK MEASUREMENTS? (Y/N)  ";Z1$
200 J1 = J1 + 1: INPUT "FILE NAME  ";Z$(J1)
210  IF Z1$ = "N" THEN  GOSUB 180: GOTO 290
220  PRINT "RETURN FOR BLANK": INPUT "";I$
230  GOSUB 180
240 N = 20
250  GOSUB 370: GOSUB 570
260  PRINT "BLANK  ";E
270  PRINT ""
280  GOSUB 180
290  PRINT "RETURN WHEN READY OR ESC FOR END": GET A$: IF A$ =  CHR$
     (27) THEN 1230
300 N = N1
305  REM  LOAD TIMERS AND START TIMING PROGRAM
310  POKE 38264,B: POKE 38290,B
320  CALL 38240
330 S = ( PEEK (38275) +  PEEK (38276) * 256) * D
340 M = R - S: PRINT  INT (M)
350  IF M > 0 THEN 330
360  GOSUB 370: GOTO 500
370  POKE 38264,B: POKE 38290,B
380  CALL 38240:B = 0:C = 0
390  FOR J = 1 TO N
395  REM  CONVERSION LOOP
400  CALL 38305
410 Y(J) =  PEEK (38361) * 256 +  PEEK (38360) - E
420 B = ( PEEK (38275) +  PEEK (38276) * 256) * D
430  IF B <  = C THEN 400
440  IF B > (C + 5) THEN B = C + D
450 Y(J) = Y(J) * P
460  PRINT Y(J),B:C = B: NEXT
470  CALL 38364
480 B = B1
490  RETURN
```

```
495  REM  DISABLE INTERRUPTS
500  CALL 38364
505  REM  SAVE DATA ON DISK
510  PRINT D$"OPEN"Z$(J1)
520  PRINT D$"WRITE"Z$(J1)
530  PRINT N: FOR J = 1 TO N: PRINT Y(J): NEXT
540  PRINT D$"CLOSE"D$(J1)
550  GOSUB 770: GOSUB 620
560  GOTO 200
570 E = 0
580  FOR J = 1 TO N
590 E = E + Y(J)
600  NEXT
610 E = E / N: RETURN
620  FOR J = 1 TO N
630 Y(J) = Z2 - (Y(J) * Z1)
640  IF Y(J) > Z2 THEN Y(J) = Y(J - 1)
650  IF Y(J) < 0 THEN Y(J) = Y(J - 1)
660  NEXT
670 Z4 = 279 / N
675  REM  DISPLAY PLOT ON MONITOR
680  TEXT : HGR2 : COLOR= 7:X = 0
690  HPLOT 0,0 TO 278,0: HPLOT 278,0 TO 278,191: HPLOT 278,191 TO
     0,191: HPLOT 0,191 TO 0,0
700  FOR J = 1 TO N
710  HPLOT X,Y(J)
720 X = X + Z4
730  NEXT
740  INPUT "";I$
750  TEXT
760  RETURN
770 T1 = 0
780  FOR J = 1 TO N
790 IN(J1) = Y(J) + IN(J1)
800  IF Y(J) > T1 THEN T1 = Y(J)
810  NEXT J
815  REM  FIND MAX AND MIN
820 SL(0) = 100:S2 = 0:S1 = 0:T = 0
830  FOR K = 1 TO L
840 XI = 1:SY = 0:XY = 0:SX = 0:X2 = 0
850  FOR J = J2 TO J3
860 SX = XI + SX
870 X2 = XI * XI + X2
880 XY = XI * Y(J) + XY
890 SY = Y(J) + SY
900 XI = XI + 1
910  NEXT J
920 UV = XY - SX * SY / J4
930 U2 = X2 - SX * SX / J4
940 SL(K) = UV / U2
950 J2 = J2 + 1:J3 = J3 + 1
960 XI = 1
970  IF M8 = 2 THEN  GOTO 1455
1000  IF SL(K) < 0 THEN  GOSUB 1190
1010  IF S2 = 2 THEN 1020
1015  NEXT K
1020 T = S1 * D
1025  REM  PRINT DATA INFORMATION
1030  PR# 5
1040  PRINT Z$(J1), INT (IN(J1)),T,E,T1
1050  PR# 0
1060 J2 = 1:J3 = J4
1070  RETURN
```

```
1080  PR# 5
1090  PRINT ""
1100  PRINT "TIME  ";R1
1110  PRINT "SAMPLING RATE MS  ";B
1120  PRINT "RUN TIME MINUTES   ";C
1130  PRINT ""
1140  IF M8 = 1 THEN  PRINT "F NAME        INTEGRAL       MAX (SEC)
      BLANK      MAX AMP"
1150  IF M8 = 2 THEN  PRINT "F NAME        INTEGRAL       MIN (SEC)
      BLANK      MAX AMP"
1170  PR# 0
1180  RETURN
1190  IF K < 4 THEN  RETURN
1200  FOR J = (K - 3) TO K
1205  NEXT J
1210  IF SL(J) > 0 THEN  RETURN : NEXT J
1220 S1 = K - 3:S2 = 2: RETURN
1230  INPUT "DO YOU WISH TO SAVE NORM INT ON FILE? (Y/N)  ";Z1$
1240  IF Z1$ = "N" THEN 1260
1250  INPUT "FILE NAME  ";Z2$
1260 T1 = 0
1270  FOR J = 1 TO J1
1280  IF IN(J1) > T1 THEN T1 = IN(J1)
1290  NEXT
1300 T1 = T1 / 1
1310  FOR J = 1 TO J1
1320 IN(J1) = IN(J1) * T1
1330  NEXT
1340  IF Z1$ = "N" THEN 1410
1350  PRINT  CHR$ (4);"OPEN"Z2$
1360  PRINT  CHR$ (4);"WRITE"Z2$
1370  PRINT J1
1380  FOR J = 1 TO J1
1390  PRINT IN(J1): NEXT
1400  PRINT  CHR$ (4);"CLOSE"Z2$
1410  PR# 5: PRINT
1420  PRINT "F NAME   INTEGRAL"
1430  PRINT : FOR J = 1 TO J1
1440  PRINT Z$(J1),IN(J1): NEXT
1450  PR# 0
1455  IF K < 4 THEN  RETURN
1460  IF SL(K) > 0 THEN  GOSUB 1500
1470  GOTO 1010
1500  FOR J = (K - 3) TO K
1510  IF SL(K) < 0 THEN  RETURN
1515  NEXT J
1520 S1 = K - 3:S2 = 2: RETURN
```

```
9560-   A9 40       LDA   #$40   ; SET BIT 6 OF ACR FOR T1 TIMER
9562-   8D 0B C1    STA   $C10B  ; FREE RUN MODE
9565-   A9 10       LDA   #$0E   ; LOAD T1 TIMER LATCH LOW BYTE
9567-   8D 04 C1    STA   $C104
956A-   A9 27       LDA   #$27   ; LOAD T1 TIMER HIGH BYTE
956C-   8D 05 C1    STA   $C105  ; AND START TIMER COUNTDOWN
956F-   A9 00       LDA   #$00   ; CLEAR MEMORY LOCATIONS FOR STORING
9571-   8D 83 95    STA   $9583  ; NUMBER OF T1 COUNTDOWNS
9574-   8D 84 95    STA   $9584
9577-   A9 C8       LDA   #$C8   ; GET SAMPLING RATE (POKED INTO
9579-   8D 85 95    STA   $9585  ; $9578 FROM BASIC)
957C-   A9 C0       LDA   #$C0   ; ENABLE INTERRUPTS
957E-   8D 0E C1    STA   $C10E
9581-   60          RTS          ; RETURN TO BASIC
9582-   EA          NOP
9583-   EA          NOP
9584-   EA          NOP
9585-   EA          NOP
9586-   EA          NOP
9587-   EA          NOP
9588-   48          PHA          ; SAVE ACCUMULATOR ON STACK
9589-   AD 04 C1    LDA   $C104  ; RESET INTERRUPT FLAG
958C-   CE 85 95    DEC   $9585  ; DECREMENT COUNTER
958F-   D0 0D       BNE   $959E  ; TIME FOR CONVERSION ?
9591-   A9 C8       LDA   #$C8   ; YES, RELOAD COUNTER
9593-   8D 85 95    STA   $9585
9596-   EE 83 95    INC   $9583  ; INC ELAPSED TIME LOW BYTE
9599-   D0 03       BNE   $959E  ; LOW BYTE FULL ?
959B-   EE 84 95    INC   $9584  ; YES. INC HIGH BYTE
959E-   68          PLA          ; RETRIEVE ACCUMULATOR
959F-   40          RTI          ; RETURN FROM INTERRUPT
95A0-   EA          NOP
95A1-   A2 00       LDX   #$00   ; MAKE PORT A OUTPUT
95A3-   8E 02 C1    STX   $C102
95A6-   CA          DEX
95A7-   8E 03 C1    STX   $C103 ; MAKE PORT B INPUT
95AA-   A9 01       LDA   #$01   ; SET MODE AND CHANNEL
95AC-   8D 01 C1    STA   $C101 ; BEFORE CONVERSION
95AF-   A9 E0       LDA   #$E0   ; RAISE CB2 HIGH IN CASE
95B1-   8D 0C C1    STA   $C10C ; IT WAS LOW
95B4-   A9 C0       LDA   #$C0   ; MAKE CB2 LOW
95B6-   8D 0C C1    STA   $C10C ; START CONVERSION
95B9-   A9 E0       LDA   #$E0   ; MAKE CB2 HIGH
95BB-   8D 0C C1    STA   $C10C
95BE-   A9 10       LDA   #$10   ; POLL IFR FOR CB1 (WAIT
95C0-   2C 0D C1    BIT   $C10D ; FOR END OF CONVERSION)
95C3-   F0 FB       BEQ   $95C0
95C5-   AC 00 C1    LDY   $C100 ; READ HIGH BYTE OF DATA
95C8-   A9 09       LDA   #$09   ; SET MODE TO RECIVE
95CA-   8D 01 C1    STA   $C101 ; LOW BYTE
95CD-   AD 00 C1    LDA   $C100 ; READ LOW BYTE OF DATA
95D0-   8C D9 95    STY   $95D9 ; STORE HIGH BYTE
95D3-   8D D8 95    STA   $95D8 ; STORE LOW BYTE
95D6-   60          RTS          ; RETURN TO BASIC
95D7-   EA          NOP
95D8-   EA          NOP
95D9-   EA          NOP
95DA-   EA          NOP
95DB-   EA          NOP
95DC-   A9 40       LDA   #$40   ; DISABLE INTERRUPTS
95DE-   8D 0E C1    STA   $C10E
95E1-   60          RTS
```

LDH Calculations

```
10  INPUT "LACTATE CONC  ";EG
20  INPUT "NAD CONC  ";EH
30  INPUT "INITIAL LDH ACTIVITY";E
32 C1 = E
35  INPUT "AMOUNT OF ENZYME INC     ";BB
40  INPUT "DELTA T IN MS      ";D1
50  INPUT "TOTAL RUN TIME IN MINUTES      ";D
60 N = D * 60000 / D1
70  DIM Y(N)
75  DIM X(N)
80  INPUT "EXCITATION MOLAR ABSORPTIVITY      ";L5
90  INPUT "EMISSION MOLAR ABSORPTIVITY      ";L8
100  INPUT "B1 IN CM       ";L6
110  INPUT "DELTA B IN CM      ";L7
120  INPUT "CONSTANT      ";L8
130  INPUT "NUMBER OF INTEGRATIONS    ";F: DIM G(F)
132  DIM T(F)
135  INPUT "DO YOU WISH TO SAVE SAMPLE CURVES ?  ":A$
136  IF A$ = "Y" THEN  GOSUB 2000
140  GOSUB 2100
142 S = 4:R = 2
147 D1 = D1 / 1000
148  PRINT "COMPLETED ITERATIONS"
150  FOR I = 1 TO F
152  PRINT (I - 1)
155 P = 0
160  REM  GET CONSTANTS
200 EA = EG:EB = EH
220 EV = 75 * E
230 EW = 1030 * E
240 E0 = 2.6 * 10 ^  - 4
250 E1 = 3.7 * 10 ^  - 2
260 E2 = 2.9 * 10 ^  - 5
270 E3 = 3.9 * 10 ^  - 6
280 E4 = 6.6 * 10 ^  - 6
290 E5 = .37 * 10 ^  - 9
300 E6 = 7.3 * 10 ^  - 9
310 E7 = 1.4 * 10 ^  - 7
320 E8 = 1.3 * 10 ^  - 9
330 E9 = 7.2 * 10 ^  - 11
335  REM  CALCULATE PRODUCT VS TIME
340  FOR J = 1 TO N
350  IF EA < 0 THEN 450
360  IF EB < 0 THEN 450
370 EN = (EV * EA * EB / E4) - (EW * EP * EP / E5)
380  IF EN < 0 GOTO 1070
390 ED = 1 + EA / E0 + EB / E1 + EP / E2 + EP / E3 + EA * EB / E4
      + EP * EP / E5 + EA * EP / E6 + EP * EB / E7
400 EX = EA * EB * EP / E8 + EB * EP * EP / E9
410 ED = ED + EX
420 EP = EN * D1 / ED
430 EP = EP + EL
440 EA = EG - EP:EB = EH - EP
450  IF EA < 0 THEN EP = EG: GOTO 480
460  IF EB < 0 THEN EP = EH: GOTO 480
470 EL = EP
480 Y(J) = EP
500  NEXT J
```

```
502 EP = 0:EL = 0
505  REM  CALCULATE FLUORESCENCE SIGNAL
510  FOR J = 1 TO N
520 LC = L8 * (10 ^  - (L5 * L6 * Y(J)))
530 LD = 1 - (10 ^  - (L5 * L7 * Y(J)))
540 LE = 10 ^  - (L8 * L6 * Y(J) / 2)
550 Y(J) = LC * LD * LE
555  IF Y(J) < Y(J - 1) THEN  GOSUB 2270
579  NEXT J
575  GOSUB 1100
580 G(I) = G(I) + Y(1) + Y(N)
705 E = E + BB
707  IF L2 > L1 THEN  GOTO 712
710  IF I = C(L2) THEN  GOSUB 800
712  NEXT I
720  PRINT  CHR$ (4);"OPEN LDH INT"
730  PRINT  CHR$ (4);"WRITELDH INT"
732  PRINT F
735  FOR I = 1 TO F
750  PRINT G(I): NEXT I
760  PRINT  CHR$ (4);"CLOSE LDH INT"
790  PRINT "RETURN FOR PRINT OUT": INPUT "";I$
795  GOTO 1000
800  PRINT  CHR$ (4);"OPEN LDH"I
810  PRINT  CHR$ (4);"WRITE LDH"I
815  PRINT N
820  FOR J = 1 TO N
840  PRINT Y(J)
850  NEXT J
860  PRINT  CHR$ (4);"CLOSE LDH"I
870 L2 = L2 + 1: RETURN
1000  PR# 5
1005  PRINT ""
1010  PRINT "NUMBER        ACTIVITY          INTEGRAL       TIME OF M
    AX"
1020  FOR I = 1 TO F
1030  PRINT I,C1,G(I),T(I)
1040 C1 = C1 + BB
1050  NEXT I
1060  PR# 0
1070  END
1100  REM  CALCULATE INTEGRAL
1110  FOR J = R TO (N - 1)
1120 P = P + 1
1130  IF P = 1 THEN X(J) = Y(J) * S
1140  IF P = R THEN X(J) = Y(J) * R:P = 0
1150 G(I) = G(I) + X(J)
1160  NEXT J
1170  RETURN
2000  INPUT "NUMBER OF CURVES TO SAVE ";L1
2010  DIM C(L1)
2020  FOR J = 1 TO L1
2030  PRINT "SEQUENCE NUMBER OF CURVE"J
2040  INPUT C(J): NEXT J
2050 L2 = 1
2060  RETURN
2100  PR# 5
2110  PRINT "LACTATE CONCENTRATION          ";EG
2120  PRINT "NAD CONCENTRATION              ";EH
2130  PRINT "LDH CONCENTRATION              ";E
2140  PRINT "ENZYME INCREMENT               ";BB
2150  PRINT "DELTA T IN MILLISECONDS        ";D1
2160  PRINT "TOTAL REUN TIME IN MINUTES     ";D
2170  PRINT "MOLAR ABS OF EXCITATION        ";L5
2180  PRINT "MOLAR ABS OF EMISSION          ";L8
2190  PRINT "B1 IN CM                       ";L6
2200  PRINT "DELTA B IN CM                  ";L7
```

```
2210  PRINT "CONSTANT                          ";L3
2220  PRINT "NUMBER OF INTEGRATIONS            ";F
2230  PR# 0
2240  PRINT "RETURN WHEN READY"
2250  INPUT "";I$
2260  RETURN
2270  IF T(I) > 1 THEN  RETURN
2280 T(I) = (J - 1) * D1
2290  RETURN
```

Glucose Calculations

```
5  LOMEM: 24576: HIMEM: 49151
10  INPUT "ENZYME ACTIVITY      ";E
15 P1 = 191
17  INPUT "NUMBER OF INTEGRATIONS  ";F
20  INPUT "INITIAL GLUCOSE CONC     ";EA
25  INPUT "GLUCOSE INCREMENT  ";BB
27 F1 = EA
30 EB = .000266
35 R1 = 1
40  INPUT "CONSTANT  ";Z
50  INPUT "DELTA T IN MILLISECONDS     ";D1
60  INPUT "TOTAL RUN TIME IN MINUTES  ";D
62  INPUT "DO YOU WISH TO SAVE SAMPLE CURVES ?  ";A$
64  IF A$ = "Y" THEN  GOSUB 600
65 C1 = 1000
66  GOSUB 1000
70 N = D * 60000 / D1
80  DIM Y(N)
82  DIM X(F)
83  DIM D(F)
84 R = 2:S = 4
90 EL = 0:EP = 0
95 EC = EB * D1 * N / C1
100 E0 = 60
110 E1 = 7 * 10 ^ 5 / E0
120 E2 = 7 * 10 ^ 4 / E0
130 E3 = 1.26 * 10 ^ 8 / E0
140 E4 = 4.1 * 10 ^ 4 / E0
150 E5 = 2.8 * 10 ^ 6 / E0
160 EG = EA:EH = EB
161  PRINT "COMPLETED ITERATIONS"
162  GOSUB 2500
165  FOR I = 1 TO F
166  IF I > 1 THEN  GOSUB 2547
167  PRINT (I - 1)
170  FOR J = 1 TO N
230  IF R1 = 0 THEN  GOTO 250
235 EP = 1 / (E1 * EA) + 1 / (E2 + E5 * EA) + 1 / (E3 * EB) + 1 /
     E4
240 R1 = E / EP
250 R2 = Z - (Z * EB / EH)
255 EP = R1 * D1 / C1
260 EQ = R2 * D1 / C1
265 EA = EA - EP:EB = EB - EP + EQ
270  IF EB > EH THEN EB = EH
275  IF EB < 0 THEN EB = EB + EP - EQ
290  IF EA <  = 0 THEN R1 = 0:EA = 0
310 Y(J) = EB
320  IF Y(J) > Y(J - 1) THEN  GOSUB 2160
330  NEXT
390  REM  DO INTEGRATION
400  FOR J = R TO (N - 1)
410 P = P + 1
420  IF P = 1 THEN X(I) = Y(J) * S + X(I)
430  IF P = R THEN X(I) = Y(J) * R + X(I):P = 0
440  NEXT J
450 X(I) = (X(I) + Y(1) + Y(N)) * D1 / (C1 * 3)
455 X(I) = EC - X(I)
460 P = 0:R1 = 1
470  IF X(I) > T THEN T = X(I)
473  IF L2 > L1 THEN  GOTO 477
475  IF I = C(L2) THEN  GOSUB 650
477 EA = EG + BB:EB = EH:EG = EA
480  NEXT I
485 T = 1 / T
```

```
490  PRINT  CHR$ (4);"OPEN GO INT"
500  PRINT  CHR$ (4);"WRITE GO INT"
510  PRINT F
520  FOR I = 1 TO F
525 X(I) = X(I) * T
530  PRINT X(I)
540  NEXT I
550  PRINT  CHR$ (4);"CLOSE GO INT"
560  GOTO 2000
590  REM  SAVE CURVES
600  INPUT "NUMBER OF CURVES TO SAVE  ";L1
605  DIM C(L1)
610  FOR J = 1 TO L1
620  PRINT J: INPUT C(J)
630  NEXT J
635 L2 = 1
640  RETURN
650 L2 = L2 + 1
660  PRINT  CHR$ (4);"OPEN G"I
670  PRINT  CHR$ (4);"WRITE G"I
680  PRINT N
690  FOR J = 1 TO N
700  PRINT Y(J)
710  NEXT J
720  PRINT  CHR$ (4);"CLOSE G"I
730  RETURN
1000  PR# 5
1100  PRINT " INITIAL ENZYME ACTIVITY      ";E
1120  PRINT " INITIAL GLUCOSE CONC         ";EA
1125  PRINT "GLUCOSE INCREMENT             ";BB
1130  PRINT " CONSTANT                      ";Z
1140  PRINT "DELTA T IN MILLISECONDS        ";D1
1145  PRINT " TOTAL RUN TIME IN MINUTES     ";D
1150  PRINT "INTEGRATIONS MADE              ";F
1160  PR# 0
1170  PRINT "RETURN WHEN READY": INPUT "";I$
1180  RETURN
2000  PR# 5
2010 EA = F1
2100  PRINT ""
2105  PRINT "NUMBER         GLUCOSE CONC         INTEGRAL        TIM
     E OF MIN"
2110  FOR I = 1 TO F
2120  PRINT I,EA,X(I),D(I)
2130 EA = EA + BB
2140  NEXT
2150  PR# 0
2155  END
2160  IF D(I) > 0 THEN  RETURN
2170 D(I) = D1 * (J - 1) / 1000
2180  RETURN
2500 X1 = 278 / N
2530  TEXT : HGR2 : COLOR= 7:X = 0
2540  HPLOT 0,0 TO 278,0: HPLOT 278,0 TO 278,191: HPLOT 278,191 TO
     0,191: HPLOT 0,191 TO 0,0
2545  RETURN
2547 X = 0
2550  FOR J = 1 TO N
2560 Y1 = P1 - (P1 * Y(J) / EH)
2570  HPLOT X,Y1
2575 X = X + X1
2580  NEXT J
2590  RETURN
```

CPK Calculations

```
5  LOMEM: 24576: HIMEM: 38233
50  GOTO 1000
98  REM  GET CONSTANTS
100 X1 = .00017
102 X2 = .0156
104 X3 = .0012
106 X4 = .00005
108 X5 = .0029
110 X6 = .0061
112 X7 = .00012
114 X8 = .018
116 V1 = .204 * E1 * 1E6 / 60
118 V2 = .111 * E1 * 1E6 / 60
120 Y1 = .00134
122 Y2 = 2.71E - 7
124 Y3 = 3.02E - 7
126 Y4 = 1.23E - 10
128 Y5 = 1.1E3
130 V3 = 75 * E3
132 V4 = 1030 * E3
134 Z1 = 2.6E - 4
136 Z2 = 3.7E - 2
138 Z3 = 3.9E - 6
140 Z4 = 2.8E - 5
142 Z5 = 6.6E - 6
144 Z6 = .37E - 9
146 Z7 = 7.3E - 9
148 Z8 = 1.4E - 7
150 S3 = 191:S4 = 278
152 G2 = 2
154  RETURN
200  REM  CALCULATE RATES
205  FOR J = 1 TO N
250 RA = V1 * A1 * A2 - V2 * A3 * A4 * X1 * X5 / (X6 * X3)
255 RB = X1 * X5 + X5 * A1 + X4 * A2 + A1 * A2 + X1 * X5 * A1 * A
    4 / (X2 * X7)
260 RC = X1 * X5 * X4 / X2 + X1 * X5 * A3 / X3 + X1 * X5 * A4 * A
    3 / (X6 * X3)
265 RD = X1 * X5 * A2 * A3 / (X3 * X8)
270 R1 = RA / (RB + RC + RD)
275 R1 = R1 / 1E6
277  IF J = 1 THEN 310
280 RA = Y1 + Y2 / B1 + Y3 / B2 + Y4 / (B1 * B2)
285 R2 = E2 / RA
287  IF J = 2 THEN 310
290 RA = (V3 / Z5) * C1 * C2 - (V4 / Z6) * C3 * C4
300 RB = 1 + C1 / Z1 + C2 / Z2 + C3 / Z3 + C4 / Z4 + C1 * C2 / Z5
      + C3 * C4 / Z6 + C2 * C4 / Z8
305 R3 = RA / RB
310 A1 = A1 - R1 * T1 + R2 * T2
315 A2 = A2 - R1 * T1
320 A3 = A3 + R1 * T1
325 A4 = A4 + R1 * T1 - R2 * T1
330 B1 = B1 - R2 * T1
335 B2 = A4
340 B3 = B3 + R2 * T1 - R3 * T1
345 B4 = A1
350 C1 = C1 - R3 * T1
355 C2 = B3
360 C3 = C3 + R3 * T1
365 C4 = C4 + R3 * T1
370 Y(J) = C3
375 T5(I) = Y(J) + T5(I)
395  PRINT Y(J)
```

```
400  NEXT J
410  FOR J = G2 TO N
415 SL(J) = Y(J) - Y(J - G2)
420  IF SL(J) > SL(J - 1) THEN G3(I) = J * T1
425  NEXT J
430  RETURN
495  REM  PLOT DATA
500  TEXT : HGR2 : COLOR= 7:X = 0
505  HPLOT 0,0 TO 279,0: HPLOT 278,0 TO 278,191: HPLOT 278,191 TO
     0,191: HPLOT 0,191 TO 0,0
507  RETURN
510  FOR J = 1 TO N
515 Y(J) = S3 - Y(J) * S1
520  HPLOT X,Y(J)
522 X = X + S2
525  NEXT J
530 X = 0: RETURN
600  PR# 1
602  PRINT "": PRINT ""
603 E1 = E4
605  PRINT "INITIAL PHOSPHOCREATINE                          "A6
610  PRINT "INITIAL ADP                                      "A5
615  PRINT "INITIAL MICRO GRAMS CPK                          "E1
620  PRINT "INITIAL GLUCOSE                                  "B5
625  PRINT "INITIAL HEXOKINASE                               "E2
630  PRINT "INITIAL NAD                                      "C5
635  PRINT "INITIAL GLUCOSE-6 PHOSPHATE DEHYDROGENASE        "E3
640  PRINT "TOTAL RUN TIME IN MINUTES                        "T2
645  PRINT "DELTA T IN MS                                    "T1
650  PRINT
655  PRINT "NUMBER          CPK                INTEGRAL"
660  PRINT
665  FOR J = 1 TO T4
670  PRINT J,E1,T5(J)
675 E1 = E1 + T3
680  NEXT
685  PR# 0: RETURN
700  DIM T7(T6)
705  PRINT "INPUT THE SEQUENCE NUMBER OF EACH CURVE TO SAVE"
710  FOR J = 1 TO T6
715  INPUT T7(J)
720  NEXT : RETURN
730  REM  SAVE CUVES
735  IF I = T7(T8) THEN 745
740  RETURN
745  PRINT  CHR$ (4);"OPEN CPK"I
750  PRINT  CHR$ (4);"WRITE CPK"I
755  PRINT N
760  FOR J = 1 TO N: PRINT Y(J): NEXT
765  PRINT  CHR$ (4);"CLOSE CPK"I
770 T8 = T8 + 1
772  IF T8 > T6 THEN T8 = 1
775  RETURN
800  PRINT  CHR$ (4);"OPEN CPK INT"
805  PRINT  CHR$ (4);"WRITE CPK INT"
810  PRINT T4
815  FOR J = 1 TO T4: PRINT T5(J): NEXT J
820  PRINT  CHR$ (4);"CLOSE CPK INT"
825  PRINT  CHR$ (4);"OPENCPK INF"
830  PRINT  CHR$ (4);"WRITECPK INF"
840  PRINT T4
845  FOR J = 1 TO T4: PRINT G3(J): NEXT J
850  PRINT  CHR$ (4);"CLOSECPK INF"
855  RETURN
1000  INPUT "INITIAL PHOSPHOCREATINE       ";A2
1010  INPUT "INITIAL ADP                    ";A1
1020  INPUT "INITIAL CPK IN MICRO GRAMS     ";E1
1025  INPUT "CPK INCRIMENT                  ";T3
```

```
1030  INPUT "INITIAL GLUCOSE                    ";B1
1040  INPUT "INITIAL HEXOKINASE                 ";E2
1042  INPUT "INITIAL NAD                        ";C1
1044  INPUT "INITIAL GLUCOSE-6-PHO DEHYDROGENASE  ";E3
1052  INPUT "TOTAL RUN TIME IN MINUTES          ";T2
1054  INPUT "DELTA T IN MS                      ";T1
1060  INPUT "MAX Y                              ";S1
1062  INPUT "NUMBER OF ITERATIONS               ";T4
1064  DIM T5(T4)
1066  INPUT "INPUT NUMBER OF SAMPLE CURVES TO SAVE  ";T6
1068  IF T6 > 0 THEN  GOSUB 700
1080 N = T2 * 60000 / T1
1082  DIM Y(N): DIM SL(N)
1084 T1 = T1 / 1000
1086 S1 = 191 / S1:S2 = 278 / N
1090 E4 = E1:T8 = 1
1095 A5 = A1:A6 = A2:B5 = B1:C5 = C1
1105  FOR I = 1 TO T4
1110  IF I = 1 THEN  GOSUB 495
1115  GOSUB 100: GOSUB 200: GOSUB 730: GOSUB 510
1130 A1 = A5:A2 = A6:B1 = B5:C1 = C5
1132 E1 = E1 + T3
1133 A3 = 0:A4 = 0:B2 = 0:B3 = 0:C2 = 0:C3 = 0:C4 = 0
1135  NEXT I
1140  GOSUB 800: GOSUB 600
```

Inflection Point Calculations

```
4 C = 15
5  DIM C(C)
7 C3 = 7
8 D = 6188
10 Z$ = "CONVOLUTION INTEGERS"
20 D$ = ""
30  PRINT "";"OPEN"Z$
40  PRINT "";"READ"Z$
50  INPUT N: FOR J = 1 TO N: INPUT C(J)
60  NEXT
70  PRINT "";"CLOSE"Z$
71  HOME : PRINT : PRINT : PRINT : PRINT "       LOAD DATA DISK": PRINT
     : PRINT
72  INPUT "NUMBER OF CURVES ";L
73  DIM X(L)
74  DIM A$(L): FOR J = 1 TO L: PRINT "CURVE-"J: INPUT A$(J): NEXT

80  HOME
90  FOR K = 1 TO L
100  PRINT "";"OPEN"A$(K)
110  PRINT "";"READ"A$(K)
120  INPUT N: IF K = 1 THEN  DIM Y(N)
125  FOR J = 1 TO N: INPUT Y(J): NEXT
130  PRINT "";"CLOSE"A$(K)
140 A = 10:B = 180
150 EP = 100
160  FOR J = A TO B
165 Y = 0
170  FOR I = 0 TO C
180 Y = Y(I + J - A) * C(I) + Y
190  NEXT I
191 Y = Y / D
195  PRINT Y,J
200  IF  ABS (Y) <  ABS (EP) THEN EP = Y:T = J + C3
210  NEXT J
220  PRINT A$(K),T
225 X(K) = T
230  NEXT K
240  PR# 5
250  PRINT "": PRINT "FILE NAME         INFLECTION": PRINT ""
260  FOR J = 1 TO L
270  PRINT A$(J),X(J)
280  NEXT
290  PR# 0
```